Chapter 11

Mesomechanics and Thermodynamics of Nanostructural Transitions in Biological Membranes Under the Action of Steroid Hormones

L.E. Panin

Additional information is available at the end of the chapter

http://dx.doi.org/10.5772/51515

1. Introduction

Biological membranes are liquid heterocrystals with low shear stability. The main structure-forming bonds in biological membranes are covalent and hydrogen bonds, and hydrophobic and weak electrostatic interactions. These bonds are responsible for high membrane elasticity – a property of particularly importance to erythrocytes, which have to pass through blood capillaries of diameter equal to the erythrocyte one. Any structural changes that increase the erythrocyte membrane viscosity hamper the motion of erythrocytes through capillaries and may result in diffuse hypoxia. In this context, of great interest is the effect of stress hormones (cortisol, adrenaline, noradrenaline) on the behavior of erythrocyte membranes.

The nonspecific binding of stress hormones with erythrocyte membranes was studied earlier in [1]. It was shown that excess of these hormones in blood are capable for nonspecific binding with blood cells, primarily with erythrocytes, producing changes in rheological properties of the blood. It was found that CO, OH, and NH active groups incorporated in the structure of hormones can form hydrogen bonds with similar groups of proteins and phospholipids of erythrocyte membranes. Hydrophobic rings of hormones can participate in hydrophobic interactions with residues of phospholipid fatty acids, as a result of which complex domains arise in the membrane structure, the membrane microviscosity increases, and the motion of erythrocytes through capillaries becomes difficult. This effect is particularly dangerous to heart because it can leads to coronary syndrome X [2, 3]. Physicians still fail to understand the nature of this phenomenon, which shows up as

exertional angina and ischemic ST segment depression on electrocardiograms with a normally functioning left ventricle.

Anabolic steroid hormones have been used for many decades, finding their most extensive use in sports medicine. Nowadays, it is impossible to train as an international class athlete without anabolic hormones. A coach's aspiration for high sporting results prompts that coach to use an ever increasing amount of anabolic steroids. Lacking a profound knowledge of sports medicine, such a coach cannot imagine all of the negative effects of anabolics on the body of an athlete. Moreover, sports medicine itself has no comprehensive information on the subject. As a consequence, the number of sudden and unexpected deaths of atheletes during the competitions has drastically increased in recent years [4].

Physicochemical analysis of the behavior of erythrocyte membranes as liquid heterocrystals makes it possible to disclose a link between structural changes in erythrocyte membranes and erythrocyte function. Of particular interest is activity of the Na+, K+-ATPhase that supports the transmembrane potential of cells and precludes their aggregation. It was previously supposed that the regulatory action of different ligands can be based on certain conformational changes of the Na^+, K^+-ATPhase [5]; however, the mechanism by which steroid hormones affect the activity of the Na^+, K^+-ATPase is poorly known.

In this work, the mechanism of testosterone, androsterone, dehydroepiandrosterone (DHEA), dehydroepiandrosterone sulfate (DHEAS) and cortisol interaction with structural components of erythrocyte membranes (mesomechanics and termodinamics of nanostructural transition) changes in their microviscosity and functional characteristics during the interaction have been studied. The results obtained could also shed light on the causes of cardiovascular catastrophes, which are often observed in sportsmen taking anabolic steroid hormones for a long time [6].

2. Materials and methods

The action of five hormones: testosterone, androsterone, dehydroepiandrosterone (DHEA), dehydroepiandrosterone sulfate (DHEAS) and cortisol (Amersham) is analyzed in the work (Fig. 1).

For this purpose, the following methods were used.

2.1. Atomic force microscopy (AFM) of erythrocytes

Erythrocytes were obtained from fresh blood after decapitation of Wistar rats under light nembutal narcosis. Blood was diluted twofold by isotonic phosphate buffer (pH 7.35) containing 0.043 M of KH_2PO_4 and 0.136 M of Na_2HPO_4. After precipitation of cells by centrifuging at 330 g for 10 min, supernatant liquor was decanted, and the washing procedure was repeated twice more.

All the procedures were performed at 4 °C [1]. The resulting erythrocyte suspension of 20 mcl volume was deposited onto a glass slide as a thin smear. The smear was predried for

10 min in air at 24 °C and humidity of 40%. After evaporation of excessive surface moisture, the smear was observed under a «Solver Bio» atomic force microscope (NT-MDT, Russia) at 24 °C using a semi-contact mode. An analogous procedure of obtaining red blood cells for the AFM examination was employed earlier by other authors [7]. In each experiment first a control specimen without hormones, and then the experimental one have been tested. Silicon cantilevers NSG11 (NT-MDT, Russia) with a resonant frequency between 120 and 180 kHz and spring constant ~ 6 N/m were used (all of these probe parameters were offered by manufacturer). Images of the surface relief of erythrocyte membrane after absorption of hormones were obtained with the scan size 1×1 μm² and 1.3×1.3 μm².

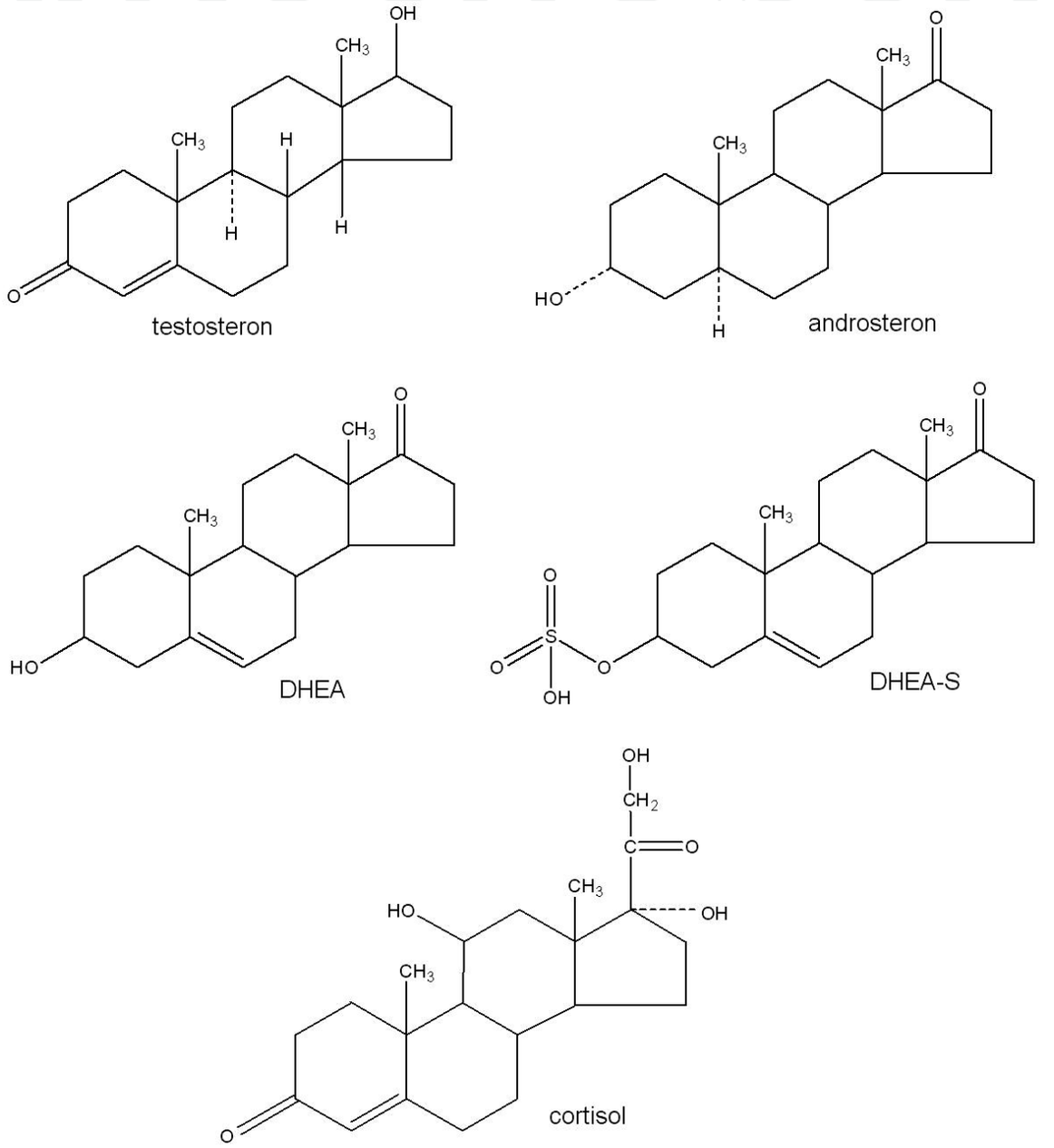

Figure 1. Chemical structure of steroid hormones.

2.2. IR spectroscopy of erythrocyte shadows

Erythrocyte shadows were obtained after their hemolysis in hypotonic phosphate buffer (pH 7.35) containing 2.75 mM of KH_2PO_4 and 8.5 mM of Na_2HPO_4. Shadows were precipitated by centrifuging at 5500 g, supernatant liquor was decanted. The washing procedure was repeated four more times [8]. All operations and further storage of shadows were performed at 4 °C.

A film for taking the IR spectra of erythrocyte shadows was prepared in a cuvette with fluorite backing via slow evaporation of water under weak vacuum at a pressure of ca. 0.1 atm (ca. $0.5 \cdot 10^4$ Pa) and temperature 4±1 °C [8]. Drying lasted 180 min. A suspension of erythrocyte shadows in a 0.001 M phosphate buffer with pH 7.35 and volume 60 mcl was introduced into a cuvette. This was supplemented with 30 mcl of the same buffer and 1.0 mcl of the hormone solution with concentration 10^{-6} M. Stirring and incubation lasted 10 min at 16-17 °C. The cuvette was placed horizontally on a special table of a vacuum unit.

When the film was prepared, the cuvette was transferred into an optical chamber and blown with dry air for 30 min, then the scanning unit was switched on. IR spectra were taken on a Specord-M80 spectrometer (Germany, Leipzig), sequentially experiment and control against the fluorite backing, or experiment and control to obtain a difference spectrum. Integration, determination of the spectrum band frequency, and mathematical processing were performed with special programs enclosed to the spectrometer. Erythrocyte suspensions were examined upon addition of cortisol using UV (Evolution 300, Thermo Scientific, USA). Merk or Sigma reagents were used in the work.

2.3. Fluorescence analysis of erythrocyte shadows

Fluorescence measurements were performed with a Shimadzu spectrofluorophotometer RF-5301(PC)SCE. 4 ml of hypotonic phosphate buffer containing 2.75 mM of KH_2PO_4 and 8.5 mM of Na_2HPO_4 (pH 7.35), and erythrocyte shadows were poured into a quartz cuvette of size $1 \times 1 \times 4$ cm^3. The concentration of shadow proteins was determined by the Warburg–Christian method from changes in the optical density of suspension [9]. On the average, it varied in the range of 0.100-0.250 mg/ml.

A cuvette with the shadow suspension was placed into a spectrofluorimeter thermostat for 1 hour. Getting a stationary temperature regime in the cuvette was controlled by an electronic thermometer. In all the experiments, temperature in the cuvette was 36 °C. After establishing a stationary temperature in the cuvette, intensity of the intrinsic fluorescence of tryptophan residues in protein membranes was measured. The tryptophan emission spectrum was taken in the range of $300 \text{ nm} \leq \lambda \leq 400 \text{ nm}$ at the excitation wavelength 281 nm, with the maximum of emission intensity observed at 332 nm. The average value of maximum emission intensity was obtained graphically after its continuous measuring for 4 minutes. Intensity of tryptophan fluorescence fluctuated within 1%. The possible reasons include variation of temperature in the cuvette with suspension, instrumental error in determination of fluorescence intensity, and photochemical reactions occurring in the

system. Spectral width of the slits was 1.5/10. The tryptophan absorption spectrum was recorded in the range of 220 nm ≤ λ ≤ 300 nm at the emission wavelength λ = 332 nm. Testosterone, androsterone, dehydroepiandrosterone (DHEA) and dehydroepiandrosterone sulfate (DHEAS) were dissolved in a mixture of dimethyl sulfoxide (DMS) and ethanol (1 : 1, V/V). Concentration of the hormone in the initial mother liquor was 10^{-3} M. If necessary, the solution was diluted with hypotonic phosphate buffer to obtain a desired concentration.

A solution of hormones with the concentration 10^{-6} M was prepared in hypotonic phosphate buffer. The time of hormone incubation with shadows was one hour. Absorption and emission spectra were taken, the average value of emission and absorption intensity was measured. For each hormone (testosterone, androsterone, dehydroepiandrosterone (DHEA) and dehydroepiandrosterone sulfate (DHEAS)), the binding constant K_b was calculated by the method [10] as well as the stoichiometric concentration of a bound hormone B_{max} and a change in free energy of the system ΔG. The interaction of hormone and erythrocyte membrane is described by the equation

$$B + nS = S_n B, \tag{1}$$

where B is a membrane protein, S is the hormone, and n is the number of moles of hormone per a mole of proteins. The binding constant K_b was calculated by the formula

$$K_c = \frac{\left[S_n B\right]}{\left[S\right] \cdot \left[B\right]}, \tag{2}$$

where $\left[S_n B\right]$ is the concentration of bound protein, $\left[B\right]$ is the concentration of free protein, and $\left[S\right]$ is the concentration of free hormone. It is supposed that hormone, upon binding to protein, completely quenches its fluorescence. Thus, the fluorescence intensity F will be proportional to the concentration of free protein. Let's write C for total concentration of protein in the cuvette, and x for concentration of the bound protein. Then,

$$\begin{aligned} F_{\max} &= \beta C \\ F &= \beta\left(C - x\right), \end{aligned} \tag{3}$$

where F is the intensity of tryptophan fluorescence at λ = 332 nm (the excitation wavelength $\lambda = 228$ nm), $F_{\max}$ is the intensity of tryptophan fluorescence in the absence of hormone (when the entire protein is free), β is the proportionality factor, and A_S is the stoichiometric concentration of hormone. When concentration of hormone exceeds A_S, the fluorescence quenching does not increase. Dividing the first equation of set (2) by the second one gives

$$x = Q \cdot C, \text{ where } Q = \frac{F_{\max} - F}{F_{\max}} \tag{4}$$

$[S] = A - n \cdot x = A - n \cdot Q \cdot C$, where A is the total concentration of hormone; $n = \frac{A_S}{C}$; $[B] = C - x = C(1-Q)$. Substitution of (2) and (3) into expression for binding constant (1) gives

$$K_c = \frac{Q}{(1-Q)(A-nQC)} \tag{5}$$

In our case, molar mass of membrane proteins is unknown, so the concentration of proteins in cuvette C is determined in mg/ml, and concentration of hormones A in mol/l. The constant n is expressed in moles of molecules of hormone per milligram of protein (M/mg) and is a ratio of the maximum concentration of bound hormone to the concentration of membrane proteins. This can be written as

$$B_{MAX} = \frac{A_S}{C} \left[{mole}/{mg\ protein} \right] \tag{6}$$

Changes in Gibbs free energy ΔG of the system upon transition of hormone from aqueous medium to erythrocyte membrane are calculated by the formula

$$\Delta G = -RT \cdot \ln(K_c) \left[{J}/{mole} \right], \tag{7}$$

where $R = 8.314 \ \frac{J}{K \cdot mole}$, and T is the absolute thermodynamic temperature.

The measurement errors appeared due to inaccuracy in volumetric dosing of the shadow suspension specimens and their titration against hormones. Specimens were dosed using pipette dispensers DPAOF-1000 and DPAOF-50, their relative error at (20±2)°C being 1% and 2%, respectively. 4 ml of the buffer was taken once with a DPAOF-1000 pipette, and suspension of erythrocytes and hormones was dosed twice using a DPAOF-50 pipette. The fluorescence intensity of erythrocyte shadows F is directly proportional to the concentrations of proteins C and hormones A in the specimen. Relative error E_F in measuring the F value can be estimated by the formula

$$E_F = \sqrt{(1\%)^2 + (2\%)^2 + (2\%)^2} = 3\%. \tag{8}$$

Relative measurement errors for K_b and B_{MAX} can be obtained in the same way. They are equal to 10%.

In calculation, the values of fluorescence intensity F were corrected for dilution of suspension after the introduction of solution with hormone, for quenching of tryptophan emission by the solvent (a mixture of DMS and ethanol), for proper fluorescence of hormones, and evaporation of water from the cuvette.

2.4. Measurement of erythrocyte membrane microviscosity

Membrane microviscosity for translational diffusion of pyrene probe was calculated as a ratio of fluorescence intensity of the pyrene dimer to fluorescence intensity of the pyrene monomer. Microviscosity of erythrocyte membranes was measured also on a Shimadzu RF-5301(PC)SCE spectrofluorimeter. The experimental specimen was prepared as follows: 4 ml of hypotonic phosphate buffer containing 2.75 mM of KH_2PO_4 and 8.5 mM of Na_2HPO_4 (pH 7.35), a fluorescent pyrene probe, erythrocyte shadows and a specified amount of hormone were placed in a quartz cuvette of size $1 \times 1 \times 4$ cm^3. Before use, all the components were stored at 4 °C. The concentration of shadow protein in the cuvette was 0.100-0.250 mg/ml; that of pyrene, $7.76 \cdot 10^{-6}$ M. Pyrene was diluted in ethanol, its initial concentration being $1.5 \cdot 10^{-3}$ M. The cuvette was placed into the spectrofluorimeter thermostat for 10 min, then the fluorescence measurements were performed at 36 °C. Before placing the specimen into the spectrofluorimeter thermostat, it was shaken vigorously for 1 min. For fluorescence measurements of shadows upon their loading with a different amount of hormones, each time a new specimen was prepared by the same procedure. Such a procedure is necessary because pyrene favors fast degradation of erythrocyte membranes.

To measure microviscosity of a lipid bilayer near proteins (the region of protein-lipid interaction), we used the excitation wavelength $\lambda = 281$ nm and spectral slit width 1.5/5. Microviscosity of a lipid bilayer far from proteins (the region of lipid-lipid interaction) was measured with the excitation wavelength $\lambda = 337$ nm and spectral slit width 1.5/3. At that, the maxima of emission intensity were observed at $\lambda = 374$ nm and $\lambda = 393$ nm (the vibronic emission peaks of excited pyrene monomers), and $\lambda = 468$ nm (the emission maximum of excited pyrene dimer).

The relative microviscosity of membranes was determined as a ratio $\eta(A)/\eta(0)$, where $\eta(A)$ and $\eta(0)$ are microviscosities of membranes, respectively, with and without hormone added to the shadow suspension. For the region of lipid-lipid interaction, relative microviscosity was calculated by the formula

$$\frac{\eta(A)}{\eta(0)} = \frac{F_{468}(0)}{F_{468}(A)} \cdot \frac{F_{393}(A)}{F_{393}(0)} \tag{9}$$

where $F_{468}(A)$ is the fluorescence intensity of pyrene at wavelength $\lambda = 468$ nm in a specimen at the hormone concentration A in suspension; $F_{468}(0)$ is the fluorescence intensity of pyrene at wavelength $\lambda = 468$ nm in a specimen with no hormone in suspension. $F_{393}(A)$ and $F_{393}(0)$ are the fluorescence intensities of pyrene at wavelength $\lambda = 393$ nm at the hormone concentration A in suspension and without hormone in suspension, respectively. The excitation wavelength is 337 nm.

For the region of protein-lipid interaction, relative microviscosity was calculated by the formula

$$\frac{\eta(A)}{\eta(0)} = \frac{F_{468}(0) - I_{468}}{F_{468}(A) - I_{468}} \cdot \frac{F_{393}(A) - I_{393}}{F_{393}(0) - I_{393}} \tag{10}$$

where I_{393} and I_{468} are the fluorescence intensities of tryptophan at wavelength $\lambda = 393$ nm and $\lambda = 468$ nm, respectively. The excitation wavelength is $\lambda = 281$ nm. A relative measurement error for relative microviscosity was equal to 6%.

2.5. Change of the Na^+, K^+-ATPase activity

Erythrocytes were extracted from fresh blood of rats. Erythrocyte suspensions with hormones of differing concentration were analyzed to activity of the Na^+, K^+-ATPhase. The experimental procedures used in these investigations are described in [5].

3. Results

3.1. Atomic force microscopy

Under atomic force microscope, erythrocytes of healthy animals looked as large biconcave discs ca. 6 μm in diameter, which agrees with the results obtained by other authors [7]. At a higher magnification, their surface showed a slight nonuniformity caused most likely by the presence of membrane proteins. When the erythrocyte suspension was supplemented with DMS and ethanol (0.25% of the mixture volume), the surface nonuniformity increased, probably due to denaturating effect of solvent on the surface structural proteins (Fig. 2). Domains with the length 200-250 nm and height 2 nm are seen. The pattern changed upon addition of testosterone to erythrocyte suspension with the final concentration 10^{-7} M (Fig. 3). The interaction of testosterone with erythrocyte membranes leads to their restructuring. The surface is tuberous, there are domains of size 400 x 400 nm and height 20-25 nm, with smaller domains on the surface of large ones: size 50 x 50 μm^2 and height 10 nm. Between them, there are regions of loosened substance that form hollows. In this case, there are pronounced distortions in the primary structure of erythrocyte membranes.

Other structural changes of erythrocyte membranes were obtained in our study upon interaction with androsterone (Fig. 4) with the final concentration 10^{-6} M. The surface is flat, there are domains of size 100 x 100 nm and height 6-8 nm. In comparison with control specimens, domains decreased in area, but increased in height.

The surface of rat erythrocyte after adsorption of DHEA is depicted in Fig. 5. Concentration of the hormone is 10^{-7} M. The surface is tuberous, there are domains of size 220 x 220 nm and height 20 -25 nm. However, they are not separated into subdomains, as in the case of testosterone.

Of the four hormones, DHEAS has the weakest effect on the membrane morphology. The surface of rat erythrocyte after adsorption of DHEAS is shown in Fig. 6. Concentration of the hormone is 10^{-7} M. The surface is flat, there are domains of size 100 x 100 nm and height 3 - 4 nm. Changes are insignificant in comparison with control. It can be suggested that DHEA

and DHEAS did not affect deep layers of the membranes, so the effect was much less pronounced. IR spectroscopy allowed us to reveal the nature of these structural transformations.

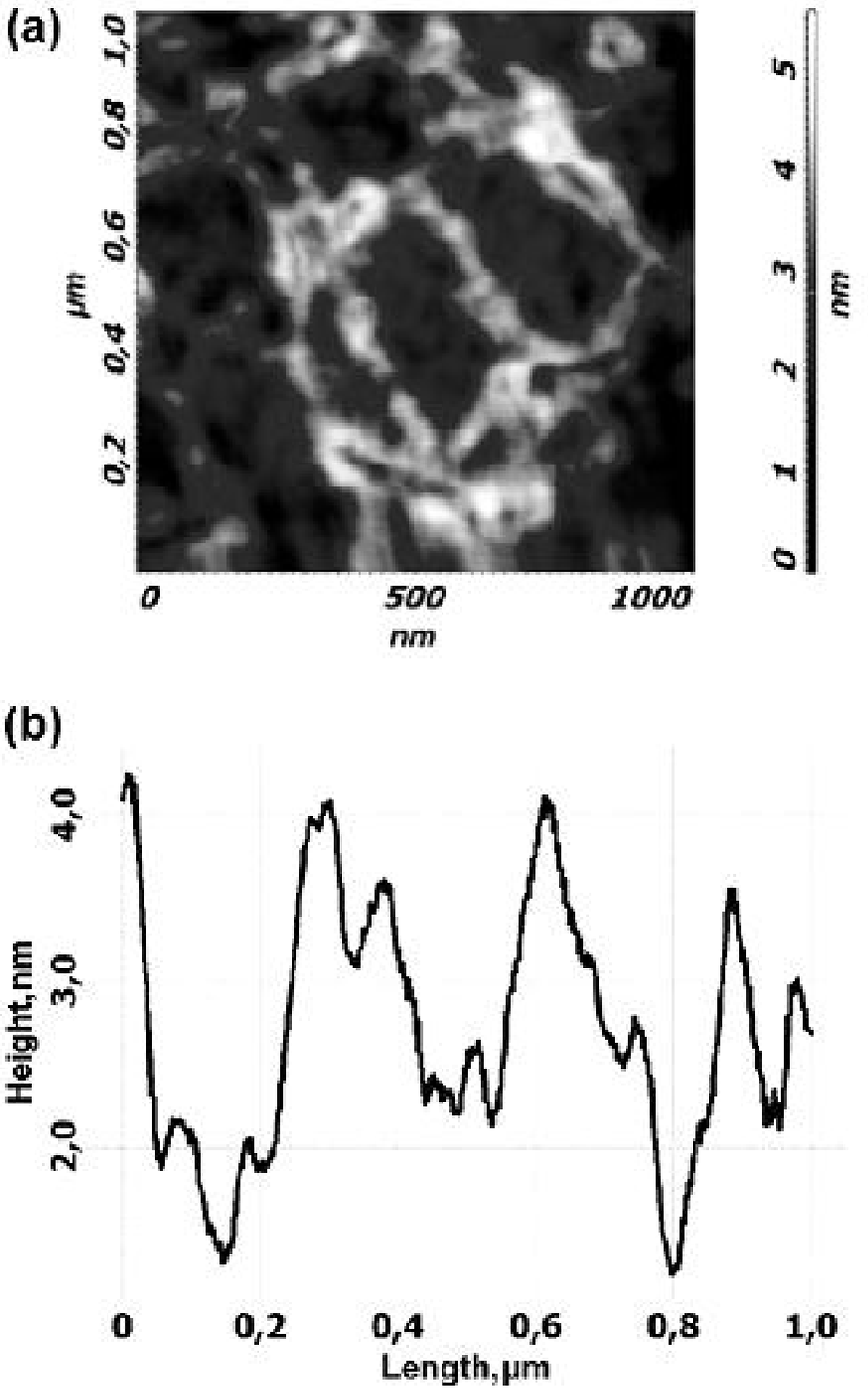

Figure 2. Control surface of rat erythrocyte. The erythrocyte suspension was supplemented with DMS and ethanol (0.25% of the mixture volume): (a) scan size 1 × 1 μm²; (b) center section of the surface.

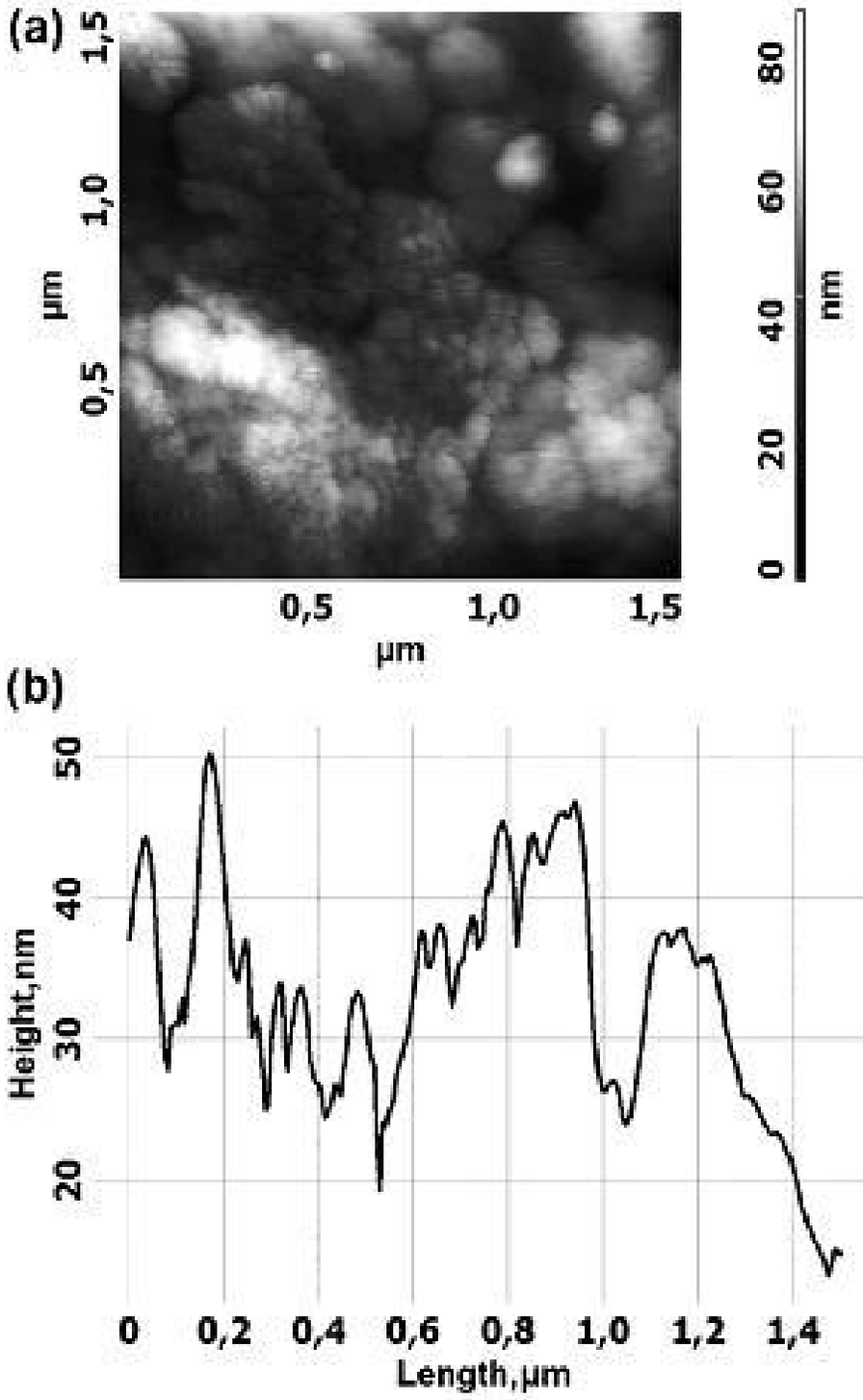

Figure 3. Surface of rat erythrocyte after adsorption of testosterone.
Concentration of the hormone is 10^{-7} M: (a) scan size 1.5 × 1.5 μm²; (b) center section of the surface.

3.2. IR spectroscopy of erythrocyte shadows

Analysis of IR spectra of erythrocyte shadows obtained from rats with no hormone loading (Fig. 7) revealed in membrane-bound proteins not only a disordered structure,

but also α-helix at 1650 and 1656 cm^{-1}, and β-structure at 1686 and 1520 cm^{-1}. Besides, we recorded NH stretching vibrations in proteins (3308 cm^{-1}), CH stretching vibrations in proteins and phospholipids (2948, 2930 and 2848 cm^{-1}), and a set of bands corresponding to phospholipids, in particular, C=O bond (1748 cm^{-1}), P=O bond (1236 cm^{-1}), CH_2 deformation vibrations (1460 and 1386 cm^{-1}), O_4C_4-C_5O_5 bond (1048 cm^{-1}) and C-C bond of deformation vibrations (978 cm^{-1}). It should be noted that C=O band (1736 cm^{-1}) is quite narrow, which gives grounds to suggest that phospholipids in membranes of normal erythrocytes are well ordered at a level of ester bonds of higher carboxylic acids and glycerol.

3.2.1. Effect of testosterone

Under the action of testosterone, intensity of absorption bands 1544, 1656 and 3292 cm^{-1} increased by 30% and more (Fig. 8, Table 1). Absorption band of NH bond showed a 3308 → 3272 cm^{-1} shift ($\Delta\nu$ = 36 cm^{-1}). The bands 2852 and 2932 cm^{-1} increased in intensity; the ratio of band intensities 2852/2932 cm^{-1} changed. The enhancement of integral intensity of the indicated absorption bands indicates an increased ordering of membrane proteins and, in particular, an increased fraction of α-helices.

The fraction of α-helices grows due to structural transition tangle → α-helix. A 3308 → 3272 cm^{-1} band shift of NH bond ($\Delta\nu$ = 36 cm^{-1}) is caused by the formation of hydrogen bond between keto group (C_3=O) in testosterone A-ring and NH bond of peptide group in membrane protein or indole ring in tryptophan. An increased intensity of the 2932 and 2852 cm^{-1} bands together with a growing intensity ratio 2852/2932 cm^{-1} confirm the rising orderliness of the entire membrane. Absorption band 1740 cm^{-1} (C=O bond of the ester group in phospholipids) increased in intensity and shifted to the short-wave region. The enhanced intensity of C=O bond reflects an increased ordering of phospholipids within domains and an increased interdomain ordering. The short-wave shift of this band is caused by the formation of hydrogen bond between OH group at C_{17} carbon atom in testosterone D-ring and C=O bond in phospholipids. Similar to segnetoelectrics a hysteresis phenomenon was observed in erythrocyte membranes [11, 12]. The spectrin-actin-ankyrin meshwork, which is connected both with membrane proteins and phospholipids, also contributes to the ordering of phospholipids. The 1088 → 1098 and 1236 → 1248 cm^{-1} shifts of absorption bands to the short-wave region result from dehydration of phospholipids due to increase in their orderliness, since the hydration process shifts these bands to the long-wave region [13] An increased intensity of bands 1098 and 1247 cm^{-1} (P-O-C and P=O bonds of phospholipids, respectively) in comparison with control specimens confirms an enhanced ordering of phospholipids under the action of the hormone.

Thus, the formation of complex domains in erythrocyte membranes upon their interaction with testosterone is caused by simultaneous interaction of CO and OH groups of the hormone with CO and NH groups both of proteins and phospholipids. In the process, water is displaced to adjacent regions, which is accompanied by membrane loosening.

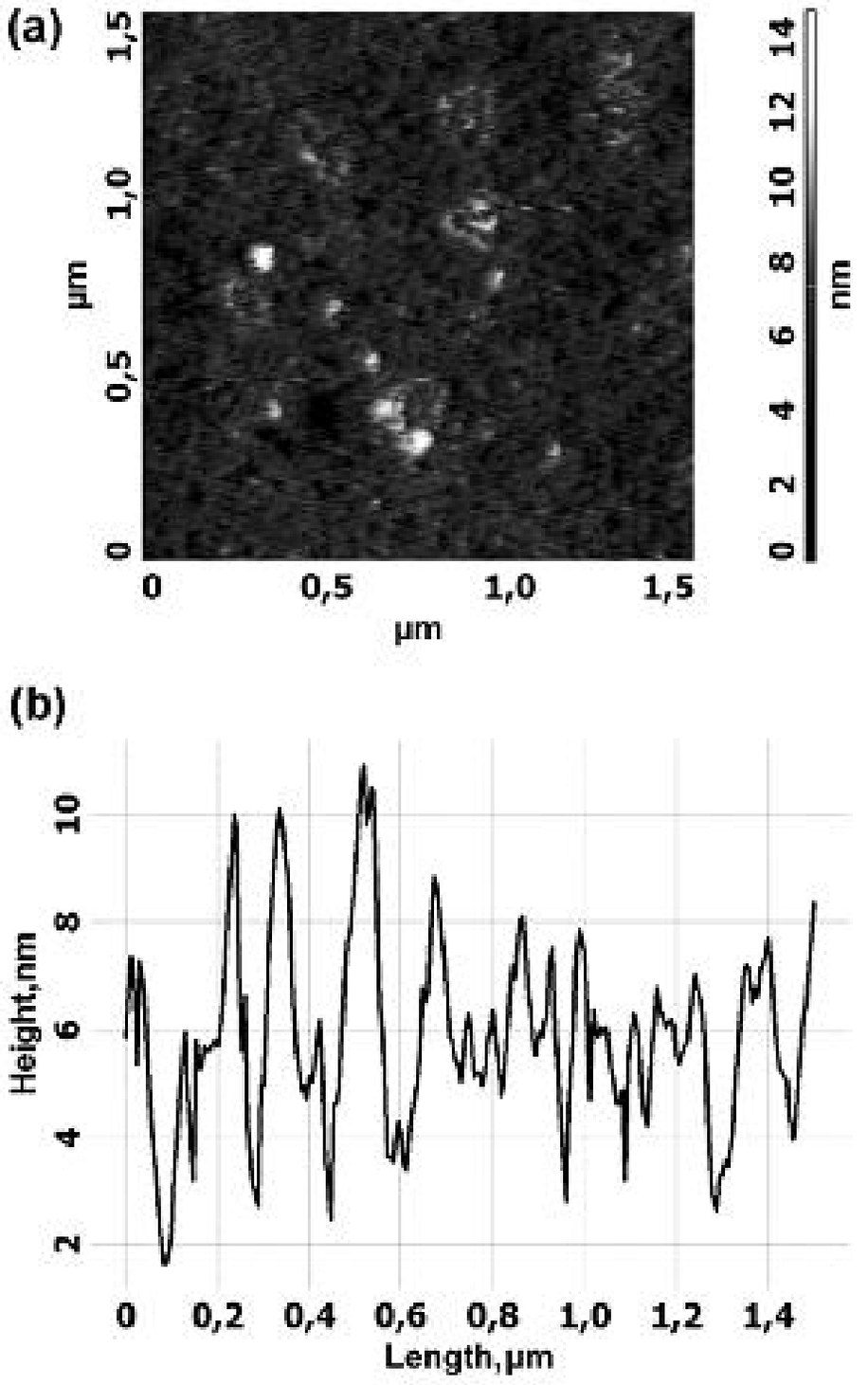

Figure 4. Surface of rat erythrocyte after adsorption of androsterone.
Concentration of the hormone is 10^{-6} M: (a) scan size 1.5 × 1.5 μm²; (b) center section of the surface.

3.2.2. Effect of androsterone

Incubation of rat erythrocyte shadows with androsterone (C_C = 2.76 x 10^{-8} M) results in shifting the frequency of NH bonds (stretching vibrations of amide A) to the long-wave

region by 38 cm^{-1} as well as shifting of NH bond of amide II ($\Delta\nu$ = 2 cm^{-1}) (Table 1). Integral intensity of absorption bands of CO (1654 cm^{-1}) and NH groups (3280 cm^{-1}) increased by 30% and more. There appeared a band at 1635 cm^{-1} corresponding to the β-structure. An increase in intensity of stretching vibrations of CH bonds at 2848 and 2930 cm^{-1} was observed. The frequency shift of NH bond is related with the formation of hydrogen bond with C_{17}=O group of the hormone D-ring. Androsterone has a more flexible structure as compared to cholesterol: its A, B and C-rings can take a more favorable conformation during the interaction with membrane proteins. Only D-ring has a flat structure, due to the presence of carbon C_{17} with sp^2 hybridization. Hydrophobic interaction with the membrane surface should also be taken into account. High conformational mobility of the molecule creates more advantageous steric conditions for hydrophobic interaction both with tryptophan, which fluorescence quenching was observed in our study, and hydrophobic regions on the membrane surface. This increases the constant of their binding to hormone and leads to more pronounced structural changes in the membranes. An increase in intensity of CO-peptide bond is related with the growing fraction of α-helices due to transition tangle →α-helix. An increase in intensity of absorption band 1620-1635 cm^{-1} is caused by structural transition tangle →β-structure. Of interest is a hypothesis stating that the indicated transitions may take place in contractile proteins, since their removal from the membrane results in a decrease or disappearance of transitions [12-13].

3.2.3. Effect of dehydroepiandrosterone

Incubation of DHEA with erythrocyte shadows showed that the frequency of stretching vibrations of NH peptide bond shifted by 20 cm^{-1} to the long-wave region (3308 →3288 cm^{-1}), whereas halfwidth of amide A decreased. An increase in the integral intensity of absorption bands at 1546, 1654.9 and 3288 cm^{-1} was observed (Table 1).

A 1236→1247.6 cm^{-1} band shift points to dehydration of phosphate groups in phospholipids. Shifting of the frequency of C=O bond in phospholipids (1748→1732 cm^{-1}) was observed; intensity of this band also increased. The 2930→2925.8 and 2848→2851 cm^{-1} shifts (CH stretching vibrations) took place, intensity of the bands increased. The intensity ratio 2852/2924 cm^{-1} changed.

3.2.4. Effect of dehydroepiandrosterone sulfate

Incubation of DHEAS with erythrocyte shadows resulted in the band shift 3308→3286 cm^{-1} (NH peptide bond) by 22 cm^{-1} (Table 1). Bands at 1548, 1656 and 3298 cm^{-1} increased in intensity with respect to control specimen; however, this was more pronounced upon addition of DHEA as compared to DHEAS. Absorption bands 1632 and 1684 cm^{-1} attributed to β-structure were observed. The band shift was recorded: 2930→2928 and 2848→2852 cm^{-1}, which was accompanied by a change in the 2852/2928 cm^{-1} ratio. The band at 1236 cm^{-1} (P=O bond) showed a strong splitting and had 3-4 bands in the region of 1236-1256 cm^{-1}. Bands at 1084 and 1100 cm^{-1} ($P\text{-}O^-$ bond) were observed. A 1748-1738 cm^{-1} shift was detected; however, it was less pronounced than in the case of DHEA addition. The DHEAS hormone

has a stronger binding with hydrophilic heads of phospholipids as compared to DHEA, and a weaker binding with membrane proteins. This suggests that DHEAS molecules cannot penetrate deep into the membrane due to their higher hydrophilicity with respect to DHEA.

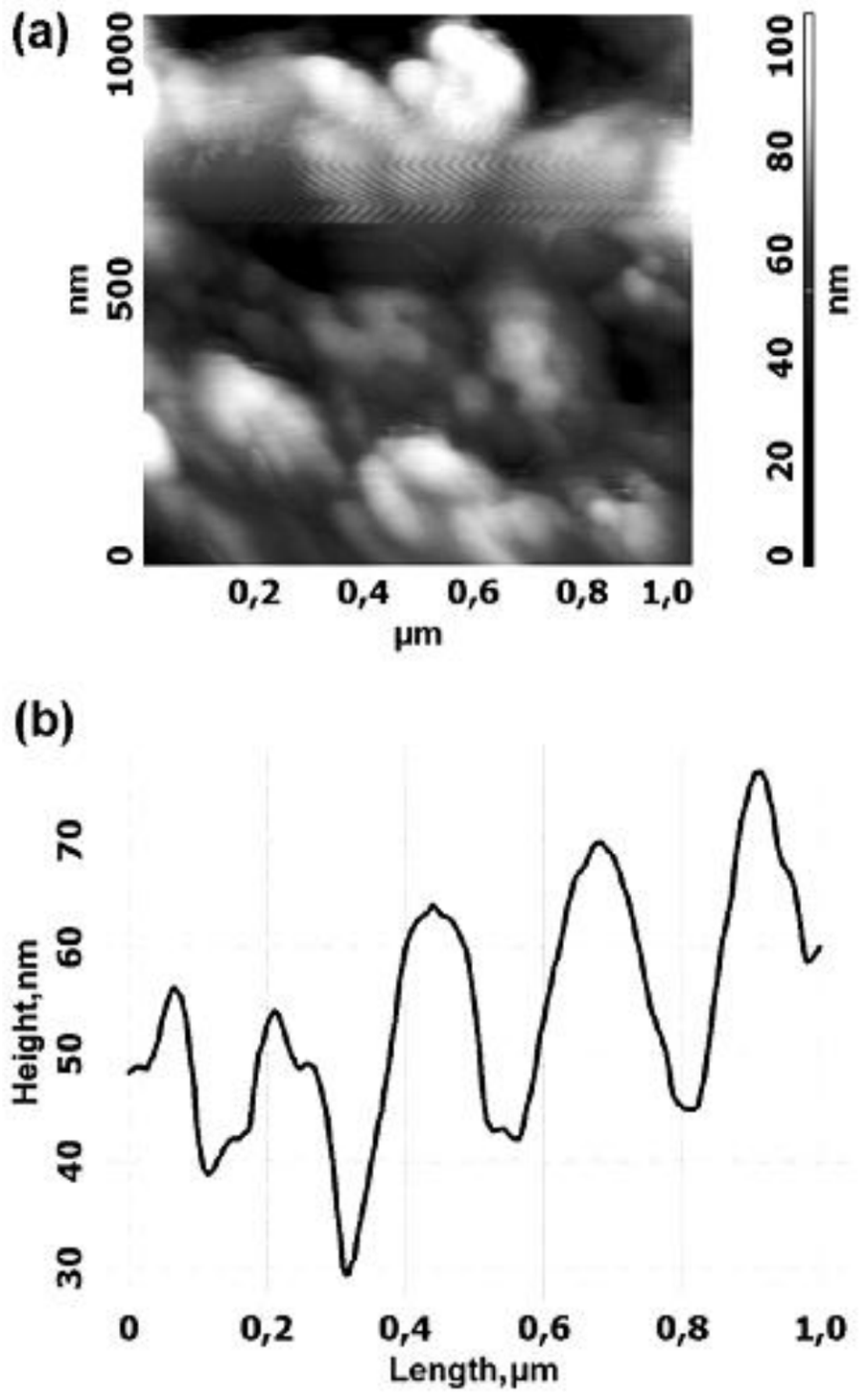

Figure 5. Surface of rat erythrocyte after adsorption of DHEA.
Concentration of the hormone is 10^{-7} M; (a) scan size 1 × 1 μm²; (b) center section of the surface.

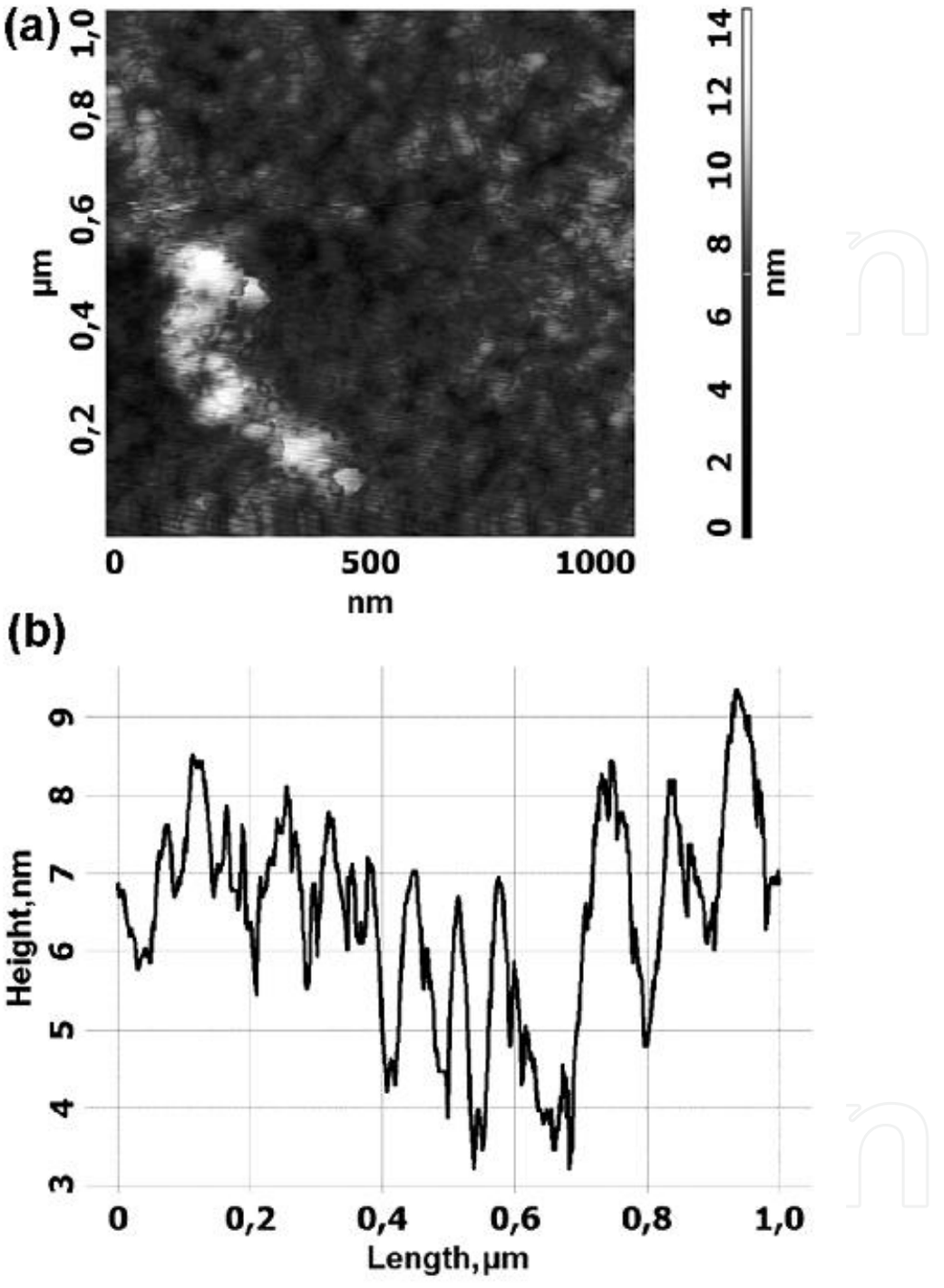

Figure 6. Surface of rat erythrocyte after adsorption of DHEAS.
Concentration of the hormone is 10^{-7} M; (a) scan size 1×1 μm^2; (b) center section of the surface.

Overall, it can be concluded that the interaction of DHEA and DHEAS with erythrocyte membranes is accompanied by the formation of hydrogen bonds between keto group (C_{17}=O) and NH group of proteins as well as between OH group at C_3 in the A-ring of the hormones and C=O group in biomembrane phospholipids. The formation of indicated

hydrogen bonds leads to ordering of membrane proteins (transition tangle →α-helix) and phospholipids. Hydrophobic interactions of hormone with the surface of erythrocyte membranes also contribute to their structural rearrangement; however, they are much less pronounced for DHEAS as compared to DHEA. The reason is that substitution of OH group by SO_3 strongly diminishes the energy of hydrogen bond, since in OH group the unshared pair of electrons is located on the oxygen atom, whereas in SO_3 group it is delocalized over the entire π-conjugated bond.

4. Fluorescence analysis

In the study, absorption intensity (D) and emission intensity (F) of tryptophan were estimated at different wavelengths. Corrections were made for dilution of erythrocyte shadow suspension after the introduction of a hormone solution, for tryptophan emission quenching by a solvent (DMS : ethanol), intrinsic fluorescence of hormones, and evaporation of water from a cuvette. To obtain a correction for solvent, the erythrocyte shadow suspension was titrated with solvent.

It was shown that solvent decreases the intensity of tryptophan absorption at $\lambda = 227.8$ nm by 33% and results in its long-wave shift to $\lambda = 230.2$ nm. Absorption intensity at $\lambda = 281$ nm changed only by 1.3% without a long-wave shifting. A maximum of emission intensity differed from control specimen also at $\lambda = 332$ nm. It did not shift upon addition of solvent, but its intensity decreased by 1.3%.

Upon addition of testosterone with the final concentration $3 \cdot 10^{-6}$ M to erythrocyte shadows, the absorption intensity at 227 nm diminished by 19 a.u. or by 2.8%; this was accompanied by an upward shift of λ to 230.4 nm. As the hormone concentration increased to $6.05 \cdot 10^{-6}$ M, the absorption intensity at 227 nm decreased by 25 a.u., or 5.0%, which was accompanied by shifting the absorption maximum to 232 nm. In the region of 280 nm, addition of hormone caused only minor changes in fluorescence. Considerable changes in the spectrum were obtained upon addition of androsterone to the shadows. Even at a concentration of $6.92 \cdot 10^{-8}$ M, which is two orders of magnitude lower compared to the case of testosterone, the absorption intensity at 227 nm decreased by 90 a.u., or 122%. It means that this hormone penetrates deeper into erythrocyte membranes than testosterone and enhances the tangle → α-helix transition in proteins, thus increasing their ordering. When erythrocyte shadows were supplemented with DHEA or DHEAS, the hypochromic effect was weak or entirely absent. A decrease in absorption intensity and a long-wave shift observed in our study can be attributed to the effect of solvent.

Analysis of the tryptophan fluorescence quenching spectra testifies that all four hormones interact with membrane-bound proteins, although a degree of this interaction differs (Figs. 9-12). The most pronounced quenching was observed in the case of androsterone (Fig. 9). The maximum fluorescence quenching was observed at a concentration of $2.2 \cdot 10^{-8}$ M. Testosterone showed a lower fluorescence quenching (Fig. 10). The maximum quenching was observed at a concentration of $1.2 \cdot 10^{-7}$ M, which is 5.5 times higher as compared to

androsterone. Fluorescence quenching was even less pronounced with DHEA (Fig. 11). In this case, the maximum quenching occurred at a concentration of $2.4 \cdot 10^{-6}$ M. And finally, the lowest fluorescence quenching was observed for DHEAS (Fig. 12). The maximum quenching took place at a concentration of $5.3 \cdot 10^{-6}$ M, which is 2.2 times higher as compared to DHEA.

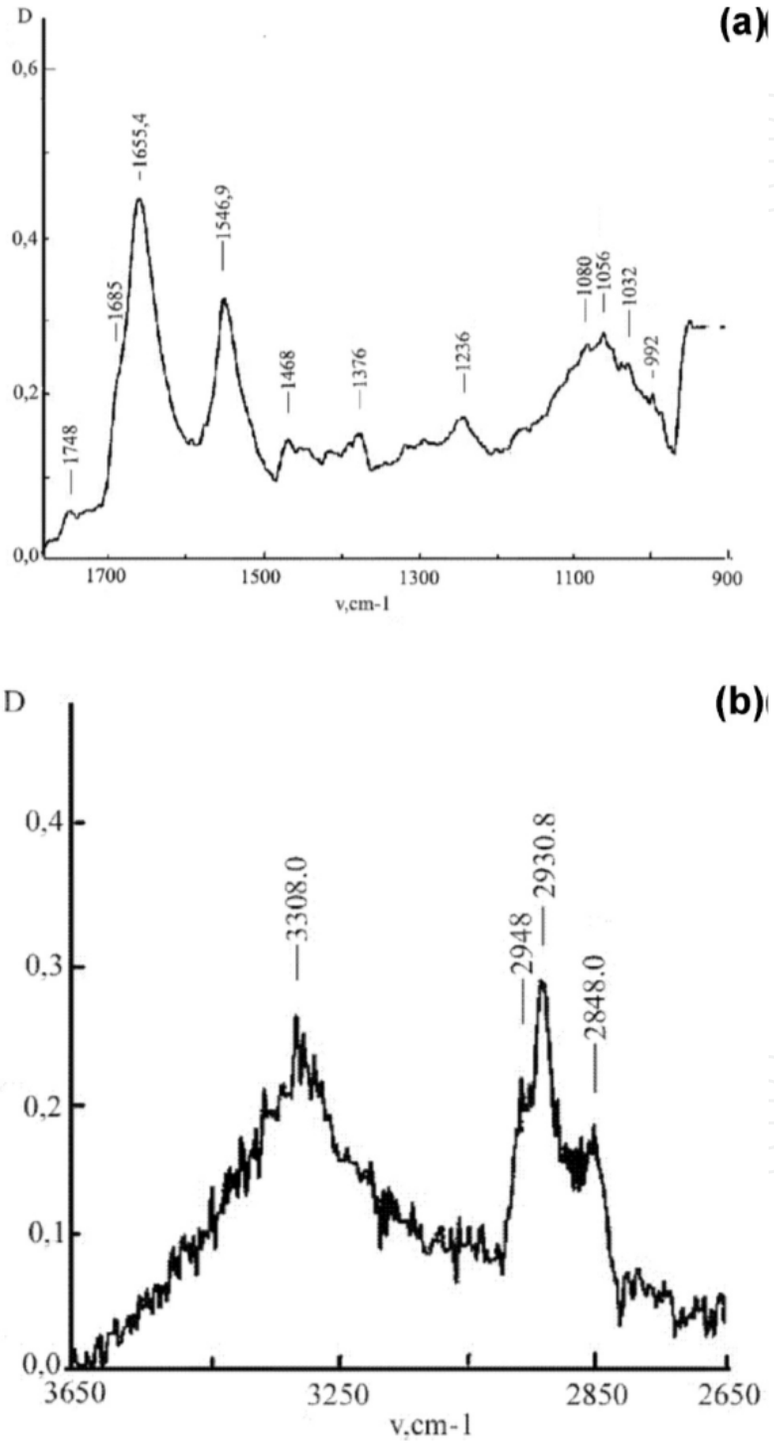

Figure 7. IR spectra of rat erythrocyte membranes (control) ($C_{phosph.buff.}$ = 0.01 M, pH 7.35, relative humidity 0%): (a) ν = 900-1800 cm^{-1}, (b) ν = 2600-3700 cm^{-1}.

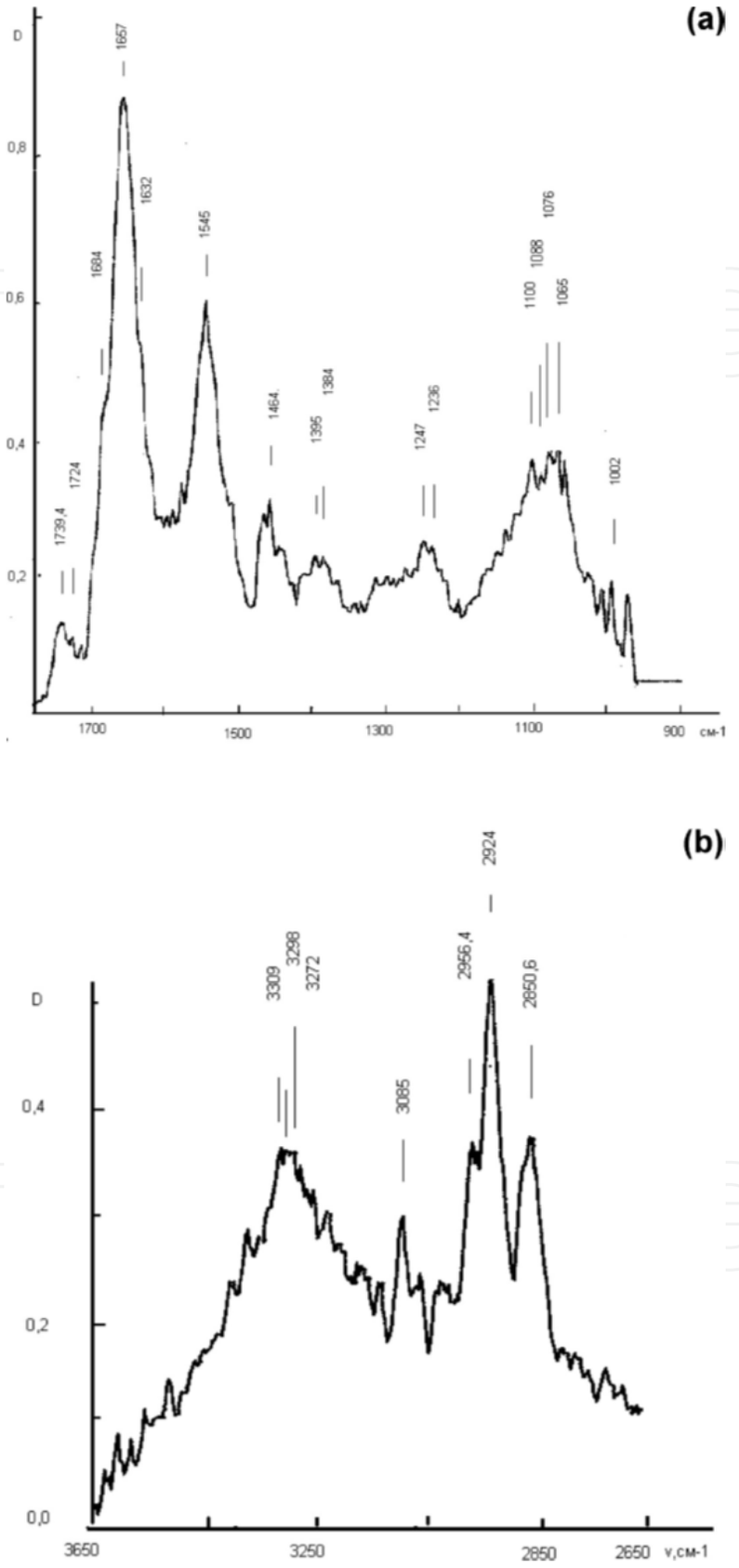

Figure 8. IR spectra of rat erythrocyte membranes incubated with testosterone (C_C = 2.7× 10^{-8} M, $C_{phosph.buff.}$ = 0.001 M, pH 7.35, relative humidity 0%): (a) ν = 900-1800 cm^{-1}, (b) ν = 2600-3700 cm^{-1}.

According to the results obtained, testosterone and androsterone penetrate deeper into erythrocyte membrane and have a stronger effect on the structure of membrane-bound proteins toward their increased ordering. DHEA and DHEAS have some effect on erythrocyte membranes; these hormones adsorb on the membrane surface, but do not penetrate deep into hydrophobic layer of the membranes. These hormones have a weaker binding with proteins via hydrogen bonds.

This conclusion is confirmed by the calculated values of hormone binding constant (K_b), total amount of bound hormone (B_{max}), and changes in free energy (ΔG) upon hormone transition from free state to the membrane-bound one (Table 2). The highest values of K_b were obtained in our study for testosterone and androsterone, K_b for androsterone being higher by a factor of 4. Amount of the bound hormone (B_{max}) obeyed an inverse relationship: it was 2.4 times higher in the case of testosterone as compared to androsterone. Changes in free energy upon interaction of hormones with erythrocyte membranes were most pronounced

Compound	ν_{CO}	ν_{NH} stretch.	$\nu_{C=O}$	$\nu_{P=O}$	ν_{P-O-C}	$\nu_{O5C4-C5O4}$	ν_{CH} stretch.	A_{CO}
Shadows (control)	1655.4 1686	3308	1748	1236	1080	1056	2948 2930 2848	1.2150 × 10
Shadows + androsterone (A = 2.76 x 10^{-8} M)	1656 1635 1620	3270 329 2		1260 1240	1098 1088		2958 2928 2848	
Shadows + testosterone (A = 2.7 x 10^{-8} M)	1657 1684 1632	3272 3298 3309	1739.4	1247 1236	1098 1088	1065 1076	2956.4 2924 2850	2.2433× 10
Shadows + DHEA (A = 2.64 x 10^{-8} M)	1654.9	3288.0	1732	1247.6	1088	1070.7	2956.3 2925.8 2851.8	2.1266 × 10
Shadows + DHEAS (A = 1.63 x 10^{-8} M)	1656.0 1680 1632.0	3286 3300 3312	1738	1248.0	1084	1070 1052.7	2952.0 2926.4 2852.0	1.2598 × 10

Table 1. IR spectroscopy. Frequency parameters of rat erythrocyte shadows after their interaction with hormones

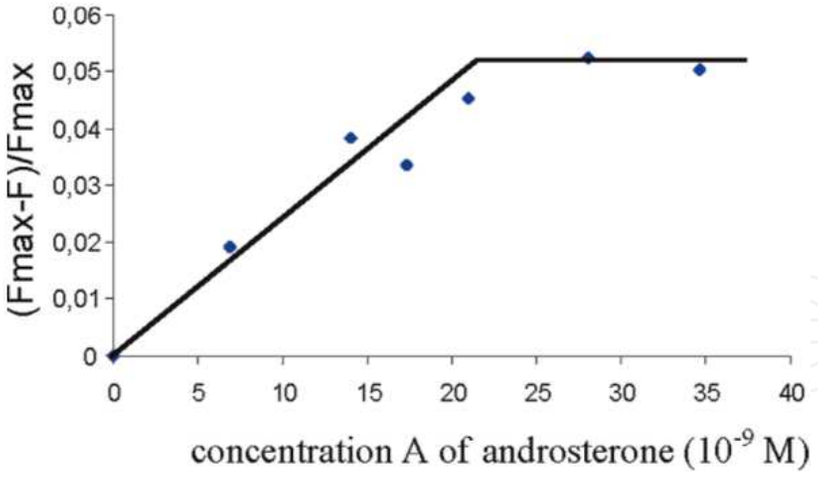

Figure 9. Q = (Fmax - F)/Fmax versus the concentration A of androsterone hormone introduced into a cuvette. Concentration of membrane protein C = 0.203 mg/mL.

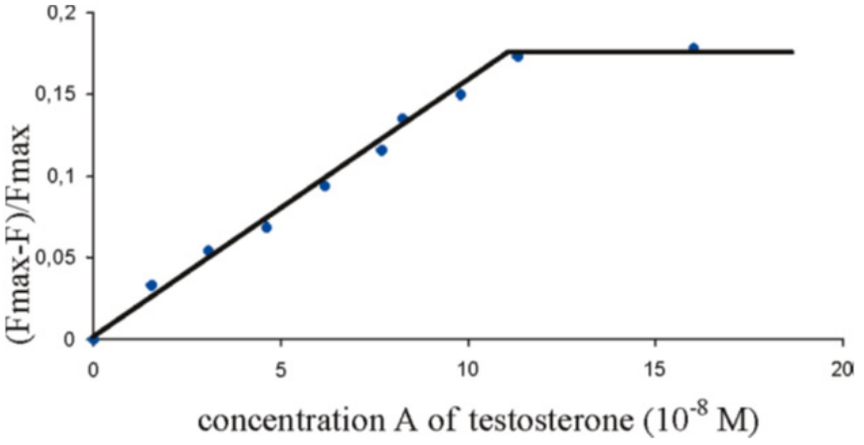

Figure 10. Q = (Fmax- F)/Fmax versus the concentration A of testosterone hormone introduced into a cuvette. Concentration of membrane protein C = 0.101 mg/mL.

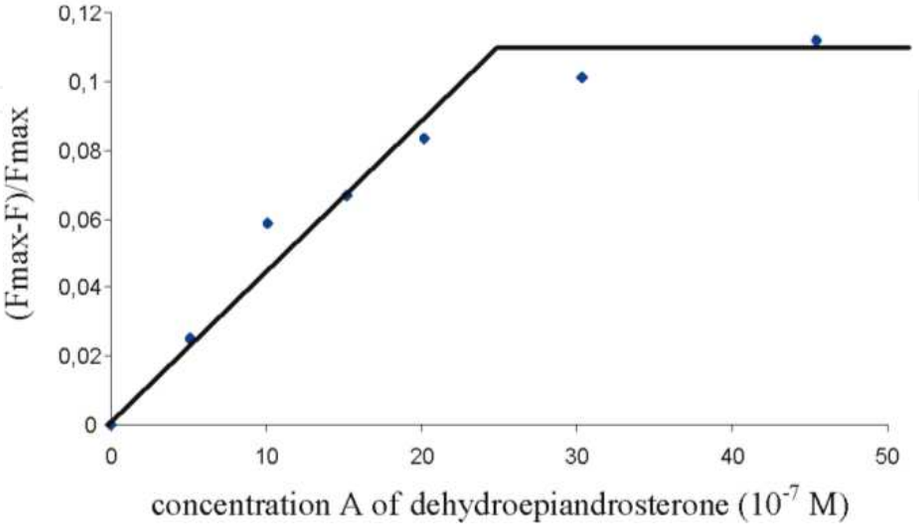

Figure 11. Q = (Fmax _ F)/Fmax versus the concentration A of dehydroepiandrosterone hormone introduced into a cuvette. Concentration of membrane protein C = 0.139 mg/mL.

All values for DHEA and DHEAS strongly differed from those listed above. Binding constants were nearly two orders of magnitude lower. Amount of the bound hormone (B_{max}) was much greater, indicating a low specificity of interaction with the membranes. Changes in free energy (ΔG) were low for both hormones (Table 2).

Thus, a comparison of two pairs of hormones demonstrated their considerable difference from each other. The higher is K_b, the greater is the binding specificity and the lower is the amount of bound hormone (B_{max}). Large negative values of ΔG for testosterone and androsterone testify that their interaction with erythrocyte membranes increases their ordering (negentropy). DHEA and DHEAS are characterized by a low specificity of binding to membranes.

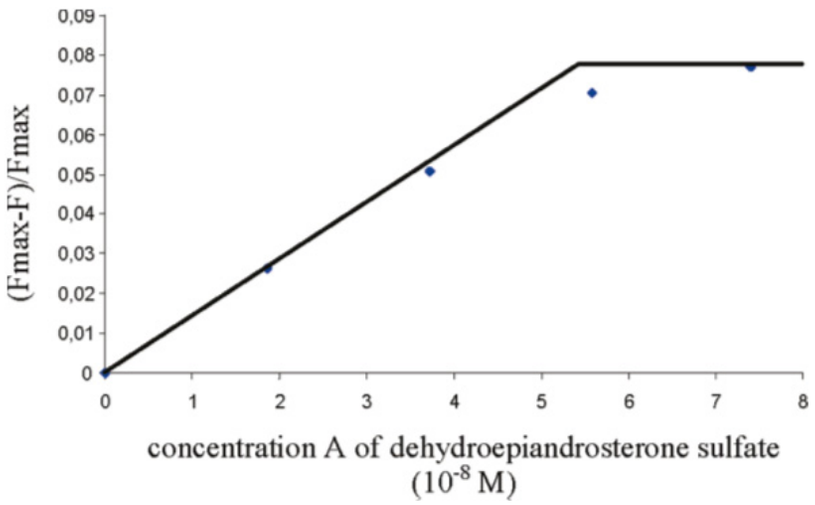

Figure 12. Q = (Fmax - F)/Fmax versus the concentration A of dehydroepiandrosterone sulfate hormone introduced into a cuvette. Concentration of membrane protein C = 0.139 mg/mL.

It shows up even when hormones are compared with each other. In DHEA, substitution of OH group by SO_3H in the 3rd position of A-ring decreases K_b by a factor of 3.8 and increases B_{max} by a factor of 2.2. A decrease in ΔG is also pronounced. The reason is that the presence of OH group and additionally of two keto groups and an S atom enhances the interaction of DHEAS with hydrophilic CO and NH groups of the surface proteins. DHEA and DHEAS cannot bind to the proteins residing in hydrophobic layer of the membrane. These two hormones do not change the conformational state of spectrin-actin-ankyrin meshwork and have only a slight effect on the morphology of membrane surface. DHEAS, being most hydrophilic among the four hormones, has the weakest effect. As hormone hydrophilicity increases, the amount of membrane-bound hormone rises and K_b decreases. During the interaction of testosterone and androsterone with erythrocyte membranes, both hydrogen bonds and hydrophobic interactions may strongly contribute to the growth of K_b. This is explained by a deeper penetration of hormones into hydrophobic layer of erythrocyte membrane, which increases the specificity of their interaction. The accompanying structural transitions in membrane proteins, tangle $\rightarrow$β-structure $\rightarrow$α-helix, increase ordering of these proteins and substantially raise the ΔG value. Results obtained in the study agree well with changes in microviscosity of erythrocyte membranes.

Steroid hormone	Binding constant K_b (M^{-1})	Amount of bound hormone B_{max} (mol/mg protein)	Changes in free energy ΔG (kJ/mol)
testosterone	$(2.24\pm0.22)x10^{6}$	$(1.09\pm0.11)x10^{-9}$	-37.6
androsterone	$(3.2\pm0.32)x10^{6}$	$(4.46\pm0.45)x10^{-10}$	-38.5
DHEA	$(5.99\pm0.60)x10^{4}$	$(1.80\pm0.18)x10^{-8}$	-28.3
DHEAS	$(1.56\pm0.16)x10^{4}$	$(4.03\pm0.40)x10^{-8}$	-24.8

Table 2. Parameters of steroid binding to erythrocyte membrane based on tryptophan fluorescence quenching of membrane proteins

5. Changes in microviscosity

In erythrocyte membrane, a fluorescent pyrene probe is distributed in the lipid phase and can be a source of information on the state of its deeper layers. The rate of its migration and the ability to form excimers upon interaction with each other are estimated. This is the way to determine changes in microviscosity of the membranes.

In our study, an increase in microviscosity was most pronounced at the addition of androsterone to erythrocyte membranes. Microviscosity started to grow at a hormone concentration of 10^{-8} M, the growth proceeding up to $2.5\cdot10^{-8}$ M with subsequent saturation (Fig. 13). The S-shaped curve points to high cooperativity in changing the conformational state of the membrane. A microviscosity increment attained 50% with respect to the initial state. In the region of protein-lipid interactions it appeared earlier and reached a higher value as compared to the region of lipid-lipid interactions. The absorption intensity (D) and emission intensity (F) of tryptophan in membrane proteins started to decrease at the same concentrations and attained a maximum also at the same concentrations (Fig. 9). Thus, our results revealed a cooperative nature of changes in erythrocyte membranes under the action of androsterone.

Addition of testosterone produced similar changes in membrane microviscosity. In the region of protein-lipid interactions, microviscosity increased at lower concentrations of hormone and attained higher values as compared to the region of lipid-lipid interactions (Fig. 14). In both cases, the revealed structural changes were initiated in proteins and carried over to lipids by virtue of cooperativity.

The effect of DHEA and especially DHEAS on erythrocyte membranes is much less pronounced as compared to testosterone (Figs. 15, 16). DHEA and DHEAS increased microviscosity by 10% with respect to initial values. In these experiments, the concentration of DHEAS reached $8\cdot10^{-6}$ M. For DHEA, the growth started at a hormone concentration of $5\cdot10^{-7}$ M and attained its maximum at $1.5\cdot10^{-6}$ M (Fig. 15). Alteration of viscosity was described by S-curve and correlated with a decrease in fluorescence and absorption of tryptophan (Fig. 11). The latter processes started at the same hormone concentrations and

reached their minima also at the same concentrations. Microviscosity in the region of protein-lipid interactions increased earlier, at lower concentrations of hormone, and was more pronounced than in the region of lipid-lipid interactions. Structural changes were initiated in proteins and involved lipids due to cooperativity.

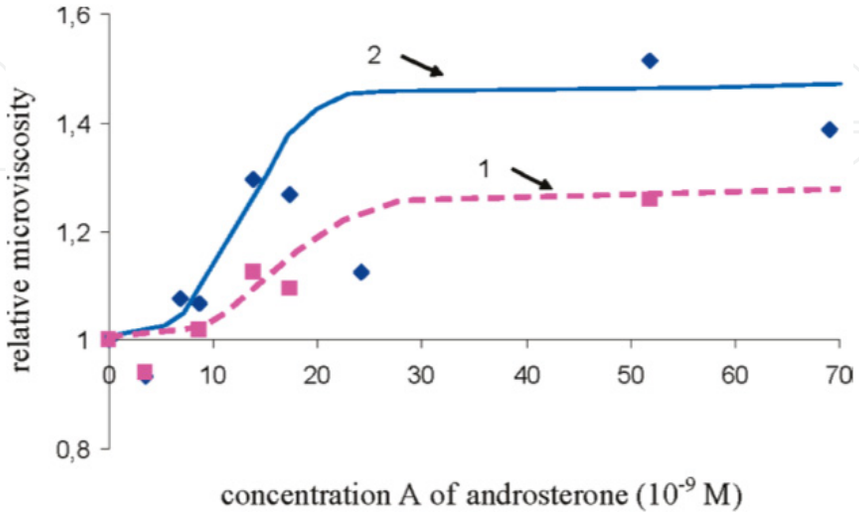

Figure 13. Changes in the relative microviscosity of membranes η(A)/η(0) of erythrocyte shadows at the concentration A of androsterone hormone. Concentration of shadows C = 0.133 mg protein/mL. Line 1 shows changes of the region of lipid-lipid interaction; line 2 – the region of protein-lipid interaction.

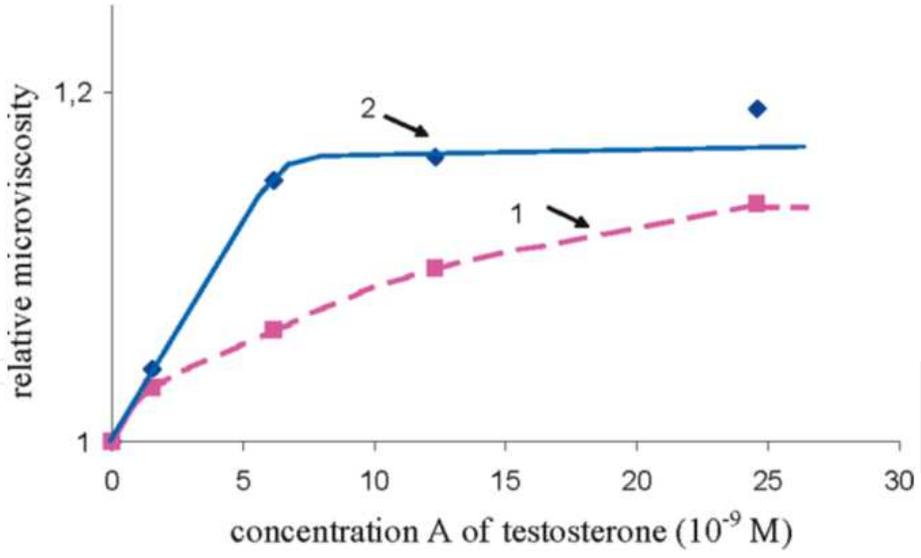

Figure 14. Changes in the relative microviscosity of membranes η(A)/η(0) of erythrocyte shadows at the concentration A of testosterone hormone. Concentration of shadows C = 0.117 mg protein/mL. 1 - the region of lipid-lipid interaction; 2 – the region of protein-lipid interaction.

The mechanism of changes in membrane microviscosity under the action of a more hydrophilic hormone DHEAS is quite different. Microviscosity goes to a constant value at a higher concentration of DHEAS in suspension as compared to that of DHEA ($5 \cdot 10^{-6}$ M versus $1.5 \cdot 10^{-6}$ M for DHEA). First changes of microviscosity appeared in the region of lipid-

lipid interactions (Fig. 16), which was followed by an increase of microviscosity in the region of protein-lipid interactions. DHEAS interacted with polar heads of phospholipids, then structural changes carried over to proteins due to cooperativity. Hydrophilic molecules of DHEAS cannot penetrate deep into hydrophobic layer of the membranes. There are only minor structural changes in the spectrin-actin-ankyrin meshwork and weak changes in membrane microviscosity.

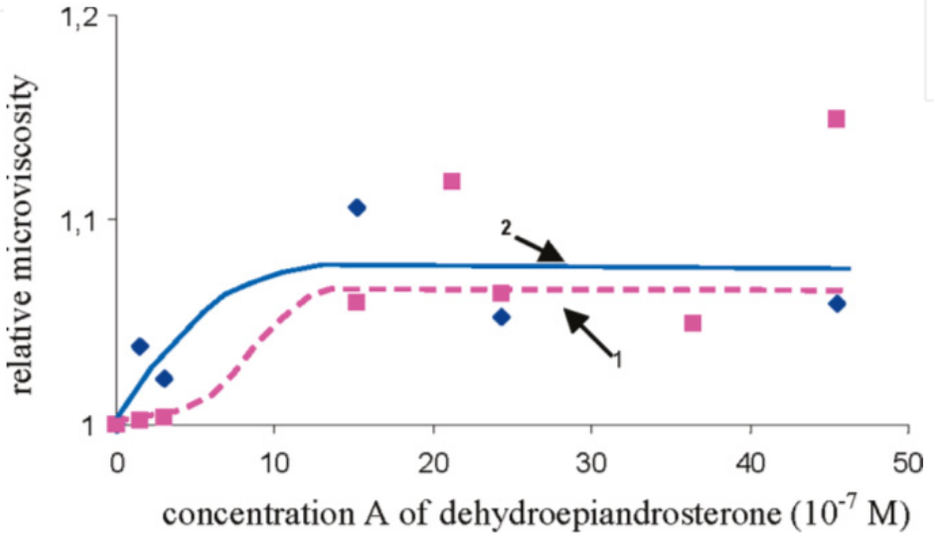

Figure 15. Changes in the relative microviscosity of membranes η(A)/η(0) of erythrocyte shadows at the concentration A of hormone DHEA. Concentration of shadows C = 0.113 mg protein/mL. 1 - the region of lipid-lipid interaction; 2 – the region of protein-lipid interaction.

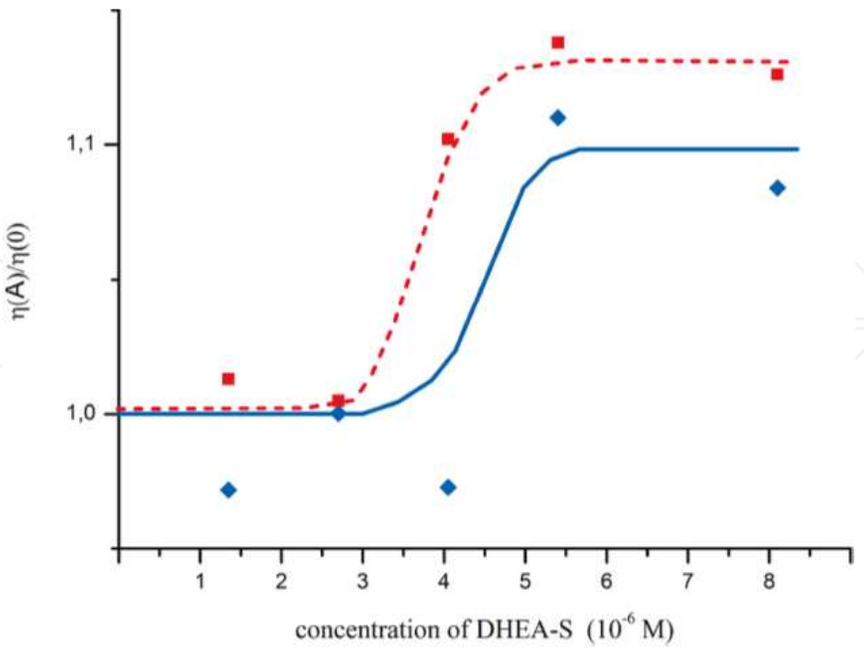

Figure 16. Changes in the relative microviscosity of membranes η(A)/η(0) of erythrocyte shadows at the concentration A of DHEAS hormone. Concentration of shadows C = 0.290 mg protein/mL. 1 - the region of lipid-lipid interaction; 2 – the region of protein-lipid interaction

6. Change of the membrane microviscosity, and Na^+, K^+-ATPase activity

Erythrocyte suspensions from fresh blood of rats with hormones of differing concentration were analyzed. For this purpose cortisol and adrenalin were used.

Under the action of hormones, the microviscosity of erythrocyte membranes increases following a saturation curve (Fig. 17). This increase depends on the hormone type and differs greatly for protein-lipid and lipid-lipid interactions. As can be seen from Fig. 17, protein-lipid interaction makes a decisive contribution to the increase in membrane microviscosity under the action of hormones. It is due to this contribution that the system of compaction domains is formed in the membrane, resulting in an increase in erythrocyte rigidity. The effect depends strongly on the hormone type. Adrenaline, which penetrates the entire erythrocyte bulk, rapidly increases the erythrocyte microviscosity, and the latter comes to saturation even at small hormone concentrations of $17 \cdot 10^{-9}$ M. Cortisol acts on an erythrocyte surface layer alone; hence, the microviscosity reaches saturation only at a cortisol concentration of $60 \cdot 10^{-9}$ M, and the increase in viscosity with cortisol is half as much as that with adrenaline.

The most important result concerns the influence of hormones on the activity of the Na^+, K^+-ATPase (Fig. 18). For both hormones analyzed, increasing the hormone concentration causes the quantity first to increase, reach its maximum, and then to decrease. The maximum of activity corresponds to the hormone concentration at which the microviscosity reaches saturation. A good correlation is found between the stages of variation in activity and in microviscosity with an increase in the concentration of different types of hormones.

Adrenaline, which is responsible for the rapid increase in erythrocyte microviscosity, is responsible as well for the rapid increase in the Na^+, K^+-ATPase activity and for its subsequent fast decline following the maximum (Fig. 18a). Increasing the cortisol concentration (Fig. 18b) causes a slow increase in microviscosity and Na^+, K^+-ATPase activity (γ), and then a slow decrease in γ whose value does remain high at a very high hormone concentration. At a $20 \cdot 10^{-9}$ hormone concentration, the activity γ is 0.05 and 0.03 μmol/h·mg protein for adrenaline and cortisol, respectively. At the stage of decline in γ at $60 \cdot 10^{-9}$ hormone concentration, γ ~ 0.02 and 0.035 μmol/h·mg protein for adrenaline and cortisol, respectively.

The maximum activity γ in the series of adrenaline and cortisol is observed at their respective concentrations of $3 \cdot 10^{-8}$ and $5 \cdot 10^{-8}$ M.

Important information on the nature of structural changes produced in erythrocytes by the analyzed hormones was obtained with infrared spectroscopy [14]. The increase in the absorption band intensity of CO- (1655.2 cm^{-1}) and NH-bonds (1548 and 3290 cm^{-1}) by about 20 % with cortisol points to enhanced ordering of membrane proteins due to the tangle → α-helix structural transition [15]. The shift 3308 → 3280 in stretching vibrations of the peptide NH-bond and the increase in its intensity owes to the formation of a hydrogen bond between cortisol and NH-bond of proteins. The increase in the absorption band intensity of

the C=O-bond of phospholipids and its shift 1748 → 1740 points to enhancement of ordering of higher carboxylic acids and to a decrease in phospholipid entropy.

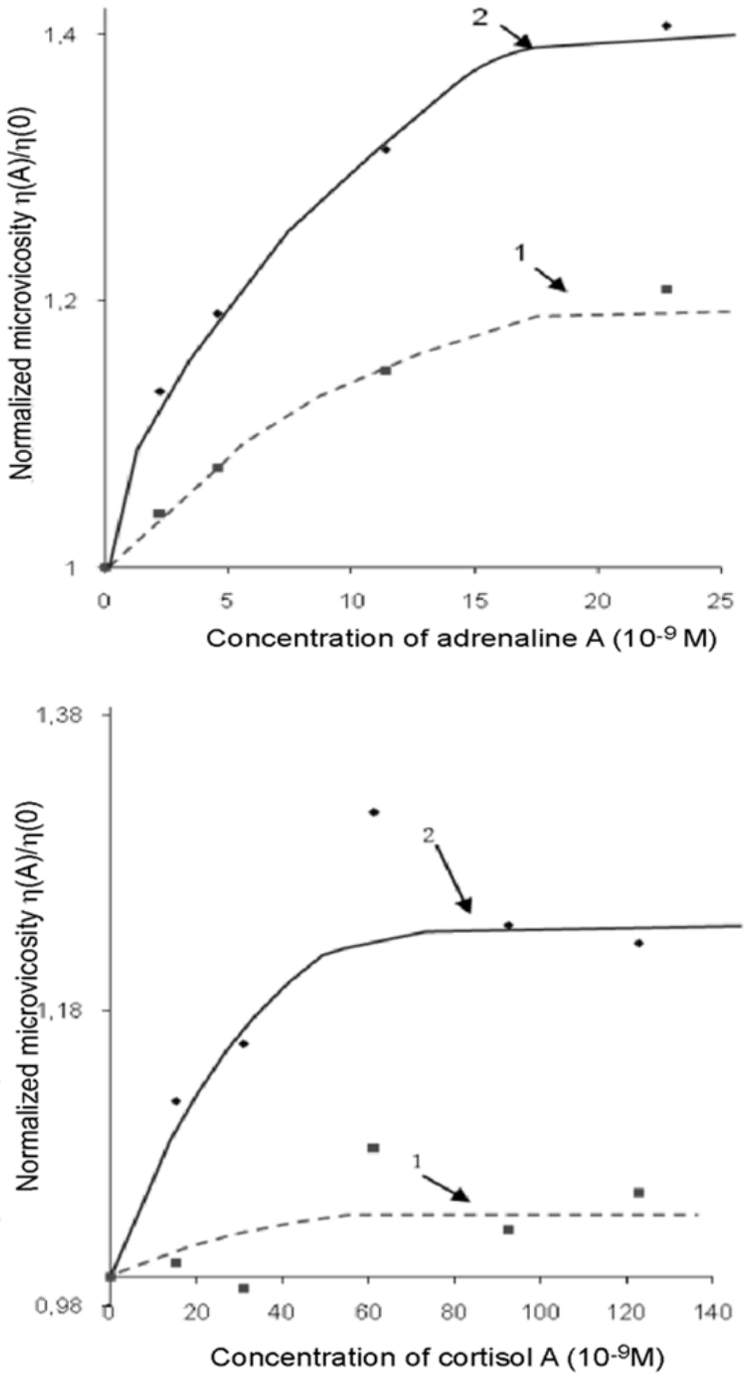

Figure 17. Changes in the relative microviscosity of membranes (L) of erythrocyte shadows at the concentration A for adrenaline (a) and cortisol (b) hormones added to the shadows suspension. Concentration of shadows C = 0.128 mg protein/ml. Concentration of pyrene in the suspension is $7.7 \cdot 10^{-6}$ M, temperature of the specimens 309.1±0.1 K (36°C), pH of the suspension 7.35. The measured value of L(A) exhibit an error of 6%. 1 - the region of lipid-lipid interaction; 2 – the region of protein-lipid interaction

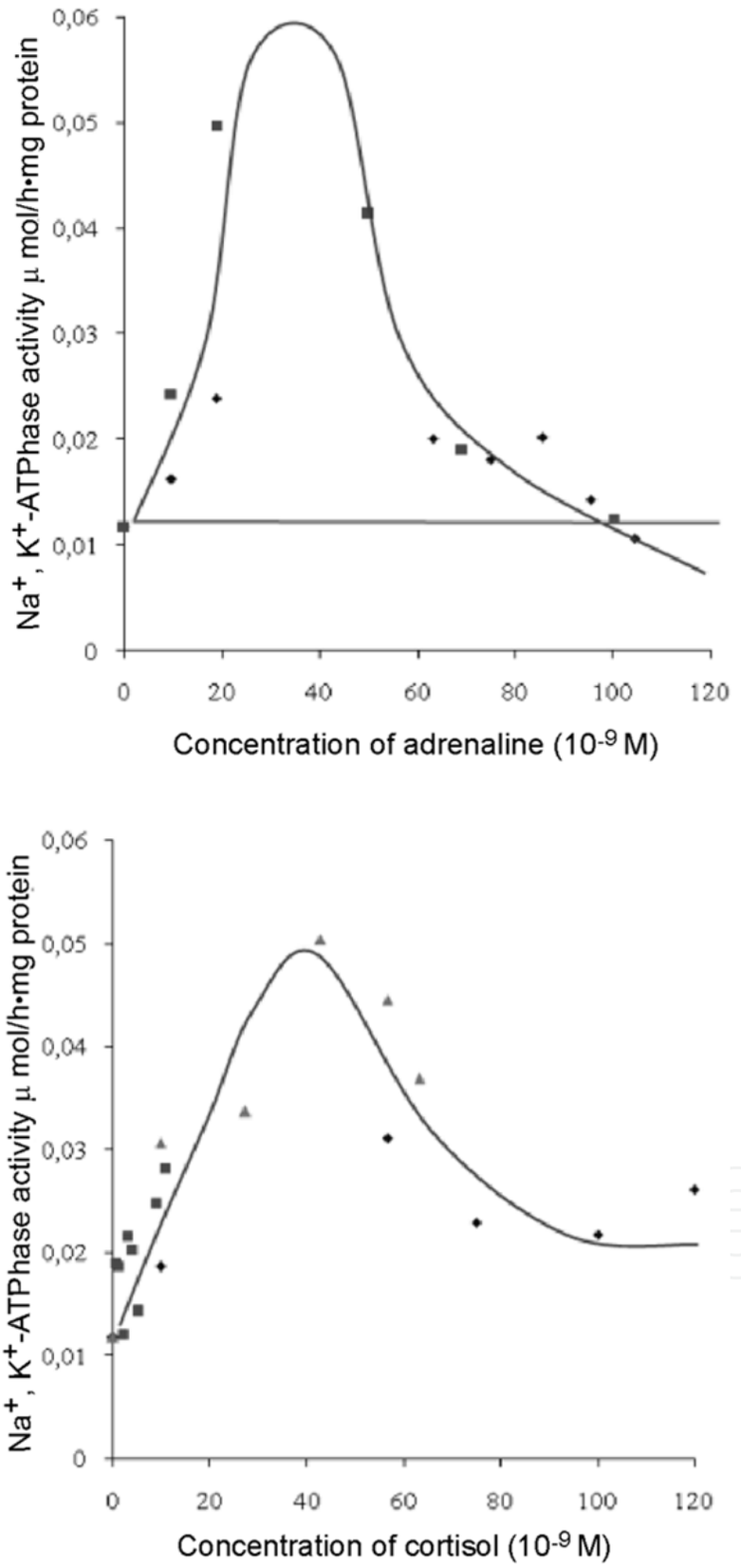

Figure 18. Changes in the activity of Na^+, K^+-ATPase of erythrocyte membranes as a function of a hormone concentration in suspension: a – adrenaline; b – cortisol.

The concurrent hormone interaction with protein and phospholipids enhances the protein-lipid interactions resulting in a complex domain structure in erythrocytes. The frequency shift of the P=O-bond toward the short-wave range and the increase in its intensity is associated with dehydration of membranes due to its hormone-induced compressive deformation. It is the loss of bound water that increases the frequency of the P = O-bond [16]. The displacement of water dipoles from protein-lipid domains to adjacent regions leads to the development of mesobands of localized deformation and discontinuities in them.

The obtained experimental results suggest that an important role in the action of hormones on erythrocytes belongs to two factors:

- collective effect of the increase in erythrocyte elastic modulus due to the formation of the domain structure in the region of protein-lipid and lipid-lipid interaction (macroscale);
- hindered structural transitions in mass transfer processes through a membrane (microscale).

The first factor causes an increase in energy quanta hν (phonone) required for structural transitions in mass transfer through erythrocyte membranes. This factor increases the activity of the Na^+, K^+-ATPase at the first stage of growth of hormone concentrations.

The second factor retards microscale structural transitions. Once the microviscosity ceases to increase (the formation of the domain structure is completed), the contribution of the first factor no longer grows, the contribution of the second factor continues to escalate, and the activity of the Na^+, K^+-ATPase decreases.

7. Effect of cortisol

Here we try to go beyond the influence of cortisol on the red cell membrane, and consider the action of the hormone on erythrocyte as a multi-layered liquid crystal system.

The mechanism of erythrocyte deformation and structural transformation of membranes and hemoglobin by the action of cortisol is still scantily investigated. The interaction of hemoglobin with contraction proteins and band 3 protein of erythrocytes is reported by Discher, D.E., Mohandas, N. & Evans, E.A [17]. These works imply that the disturbance and deformation of erythrocyte membrane caused by cortisol or other external factors can be transferred to hemoglobin by means of band 3 integral protein or contraction proteins. According to modern ideas, contraction proteins reside as at the inner as outside of membrane. Within this concept, a reverse response is also possible, i.e., the disturbance can be transferred from hemoglobin to the cell membrane.

The addition of cortisol to erythrocyte suspension with the hormone concentration of 10^{-8} to $6{\cdot}10^{-8}$ M produced a set of UV spectral curves. A maximum of absorption band at 418 nm was shown to decrease with increasing the hormone concentration. A decrease in the optical density was 22% as compared to erythrocyte suspension without hormone (control) (Fig. 19). The resulting set of curves was used to plot the dependences of optical density for band 418 nm on the concentration of hormones.

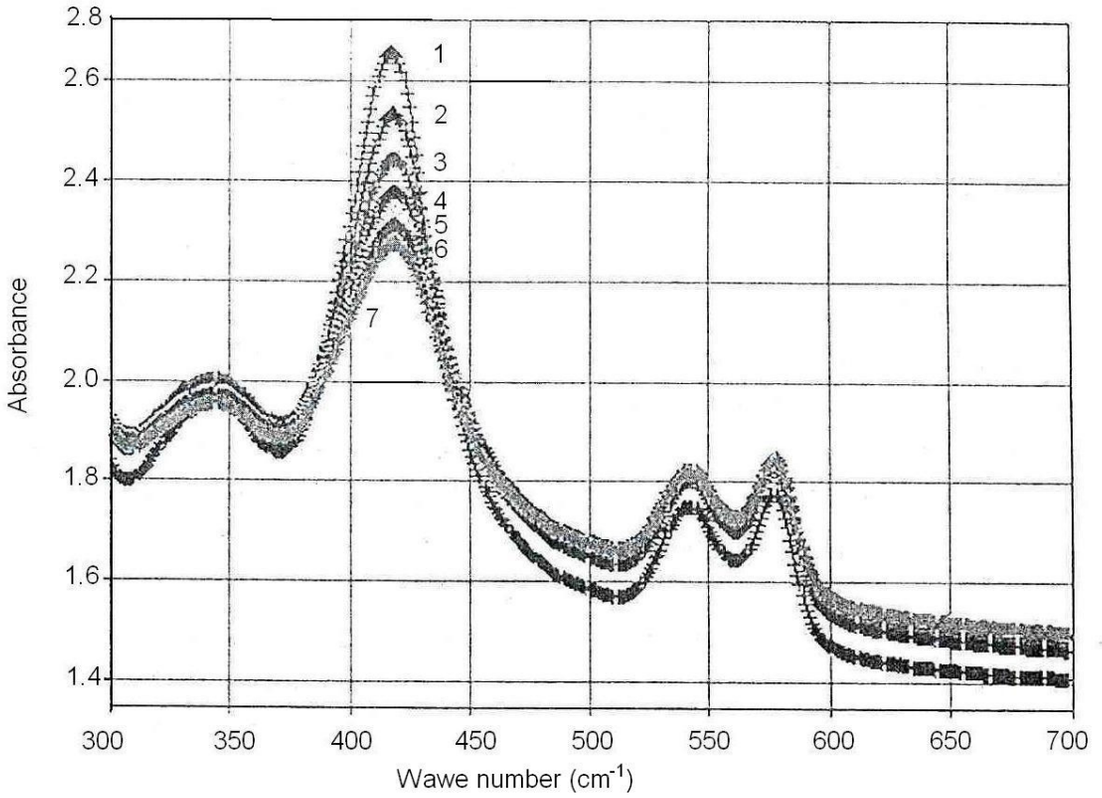

Figure 19. Changes in the optical density of absorption band 418 nm at the addition of cortisol to human erythrocyte suspensions ($C = 10^{-8} – 6 \cdot 10^{-8}$ M).

An increase in the optical density in the regions of 600-700 and 310 nm, which points to increasing diffusion of light has been also observed. In these regions, optical density changed by ~5.5%, which considerably exceeds the measurement error (0.5%) (Fig. 19). It should be noted that absorption band at 418 nm may shift spontaneously by ± 2-3 nm in different runs, generally to the short-wave region. Shifting of this band occurs either due to fluctuations in the structure of hemoglobin itself [18] or by the action of fluctuations in the structure of membrane and cell as a whole [19, 20].

The analysis of IR spectra of rat erythrocyte ghosts not loaded with hormone (control, Fig. 7) revealed not only a disordered structure, but also the presence of α-helix 1650-1656 cm^{-1} and β-structure (1686 and 1520 cm^{-1}) in the proteins of rat erythrocyte ghosts [1]. NH stretching vibrations of proteins (3308 cm^{-1}), CH stretching vibrations of hydrocarbon chains in proteins and phospholipids (2948, 2930 and 2848 cm^{-1}) as well as some bands typical of phospholipids, in particular, C=O bond (1748 cm^{-1}), P=O bond (1236 cm^{-1}), CH_2 deformation vibrations (1460 and 1386 cm^{-1}) of hydrocarbon chains, O_4-C_4-C_5-O_5 bond (1048 cm^{-1}) of monosaccharides in glycolipids and glycoproteins, and C-C deformation vibrations (978 cm^{-1}) have been recorded. Note that the C=O band (1736 cm^{-1}) is quite narrow; hence it follows that phospholipids are well ordered at the level of ester bonds in higher carboxylic acids and glycerol.

Analysis of the IR spectra of rat erythrocyte ghosts upon incubation with cortisol at its concentration of $4.4 \cdot 10^{-8}$ M revealed a ca. 20% increase in intensity of the absorption bands

of CO (1655.2 cm^{-1}) and NH bonds (1548 and 3290 cm^{-1}), the effect building up with an increase in the hormone concentration (Table 3, Fig. 20). A growing intensity of the band 1655.2 cm^{-1} testifies an increase in the fraction of α-helix [8]. The increasing fraction of α-helices in membrane proteins is related with the structural transition tangle → α-helix.

A shift of NH bond (stretching vibrations of peptide bond, 3308 ⟶3280 cm^{-1}, $\Delta\nu = 28$ cm^{-1}) was accompanied by a growth of its intensity, which is related with the formation of hydrogen bond between cortisol and NH group. Hydrogen bond is likely to form between keto group of A-ring (C_3=O) and NH group of the membrane protein. Meanwhile, keto group (C_{20}=O) of D-ring and OH group at C_{11} in C-ring could also be involved in the formation of hydrogen bonds. The presence of several hydrophilic groups strongly changes the biological activity of cortisol and other steroid hormones, in distinction to cholesterol. Cholesterol binds to phospholipids mainly due to hydrophobic interaction (Van der Waals forces) with fatty acid residues [19]. Shifting of CH bond stretching vibrations 2848 → 2852 cm^{-1} ($\Delta\nu = 4$ cm^{-1}) and 2930 → 2925 cm^{-1} ($\Delta\nu = 5$ cm^{-1}) were observed. The latter increased in intensity under the action of hormone. Changes in intensity of this band confirm the presence of structural transition, but cannot differentiate the place where the transition occurs — in membrane proteins or in phospholipids, as CH bond is present both in proteins and phospholipids. However, as seen from our experimental data, this band reflects mainly the changes in phospholipid orderliness.

An increase in intensity of the absorption band of phospholipid C=O bond and its shift 1748 → 1740 cm^{-1} were observed. This increase of the band intensity indicates a growing orderliness of higher carboxylic acids and a decreasing entropy in phospholipids. Shift of the band is related with the formation of hydrogen bond between hormone, for example OH group at C_{21}, and CO bond of phospholipids. Such interaction of the hormone simultaneously with protein and phospholipids can occur at the interface between protein and phospholipids, i.e., in a near-boundary or annular layer of the band 3 integral protein, glycophorin and other proteins.

P=O bond shifted in frequency by 3 cm^{-1} to the short-wave region and increased in intensity. Shifting of P=O bond to the short-wave region is attributed to dehydration of membranes during their deformation under the action of hormone. A loss of bound water increases the frequency of P=O bond [1]. Deformation (contraction) occurs due to spectrin-actin and spectrin-ankyrin networks [19], since the extraction of spectrin from membrane relieves the deformation caused by hormones. It should be noted that 30% of membrane proteins is represented by spectrin. Overall, contraction proteins constitute 55-60% of all membrane proteins [21]. Steroids can attack either the spectrin-actin-ankyrin network located both on internal and external surfaces of the membrane or the integral proteins associated with contraction proteins [22].

Our FTIR spectroscopy study of the hormone effect on intact erythrocytes revealed considerable changes of the spectra in absorption regions both of proteins and phospholipids. In particular, cortisol gave rise to absorption band 1636 cm^{-1} corresponding to β-structure of membrane proteins, which indicates a transformation in the secondary

structure of membrane proteins (tangle → β-structure transition) involving also the contraction proteins. Shifting of some other absorption bands attributed both to proteins and phospholipids was observed too (Fig. 21).

Noteworthy are the shift of absorption band 2870 cm^{-1} corresponding to stretching vibrations of CH bond in hemoglobin [23], and a more pronounced splitting in the region of stretching and deformation vibrations of phospholipid CH orderliness in and between the domains. A stronger splitting of CH bonds testifies the formation of new lipid-protein clusters as a result of intermolecular interaction, due to compaction of membrane elements caused by structural transformation of the contraction proteins network. In our earlier studies of high density lipoproteins (HDL), when calculating the enthalpy of structural transitions from experimental data, the occurrence of smectic A → smectic C transition in HDL phospholipids [8] has been suggested. Such a transitions may occur here, since it has a low enthalpy [8, 24].

Of interest is the appearance of the absorption band 2851.8 cm^{-1}, which is assigned to stretching vibrations of CH bond in phospholipids [8]. This band results from structural transition in membrane phospholipids.

No.	The object of measurement	νCO	νNH val.	νC=O	νP=O	νP-O-C	ν05C4-C504	νCH val.	ACO
	Ghosts (control)	1655,4 1686	3308	1748	1236	1080	1056	2948 2930 2848	1,2150E + 01
2	Ghosts + cortisol (C= 4,4·10^{-8} M)	1655,2	3290,4 3308.0	1743 -	1236	1080	1051,2	2924,2 2848,9	1,5169E + 01
3	Ghosts + cortisol (C= 10^{-7} M)	1656,0 1630	3280 3300	1740	1239	1083,7	-	2962 2925 2852	1,5640E + 01
4	Erythrocytes (control)	1649,9	3282,1 3272,0		1245,7	1106,2		2956,8 2935,8 2871,7 3030,2	
5	Erythrocytes + cortisol (C= 10^{-8} M)	1642,7 1627,5	3285,3 3270,2 3247,3	1741,1 1707,5	1239,4 1201,3	1100,0 1089,5	1060,2	2956,6 2937,5 2872,3 3028,4 3052,4	

Note. ACO is the integral intensity of absorption band νCO of the peptide bond in semilogarithmic form.

Table 3. Frequency characteristics of human erythrocytes and rat erythrocyte ghosts before and after their interaction with hormones

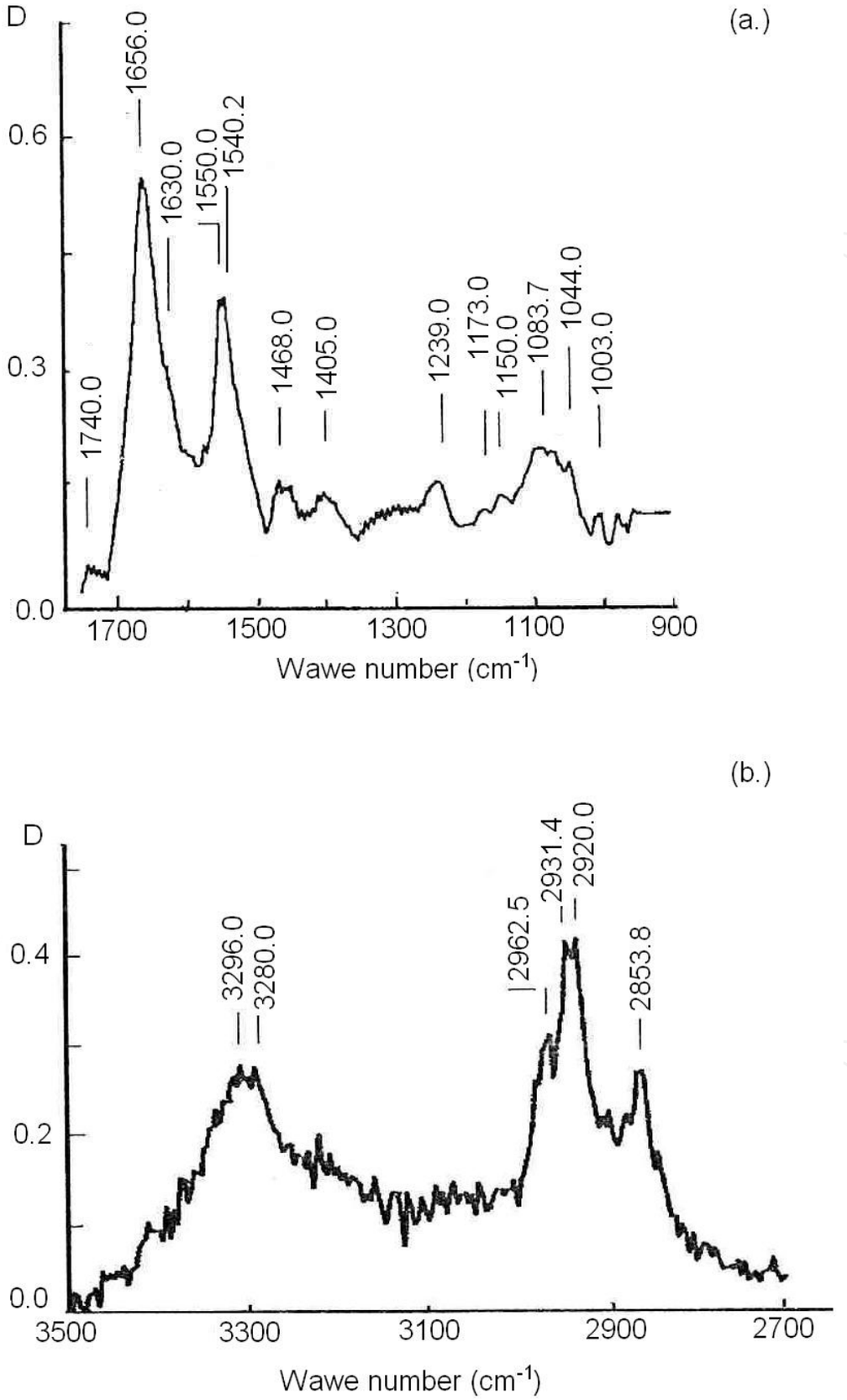

Figure 20. IR spectraof rat erythrocyte ghosts at the addition of cortisol (C = 4.4· 10^{-8} M): a. - ν = 1000 – 1800 cm^{-1}, b. - ν = 2600 – 3400 cm^{-1}.

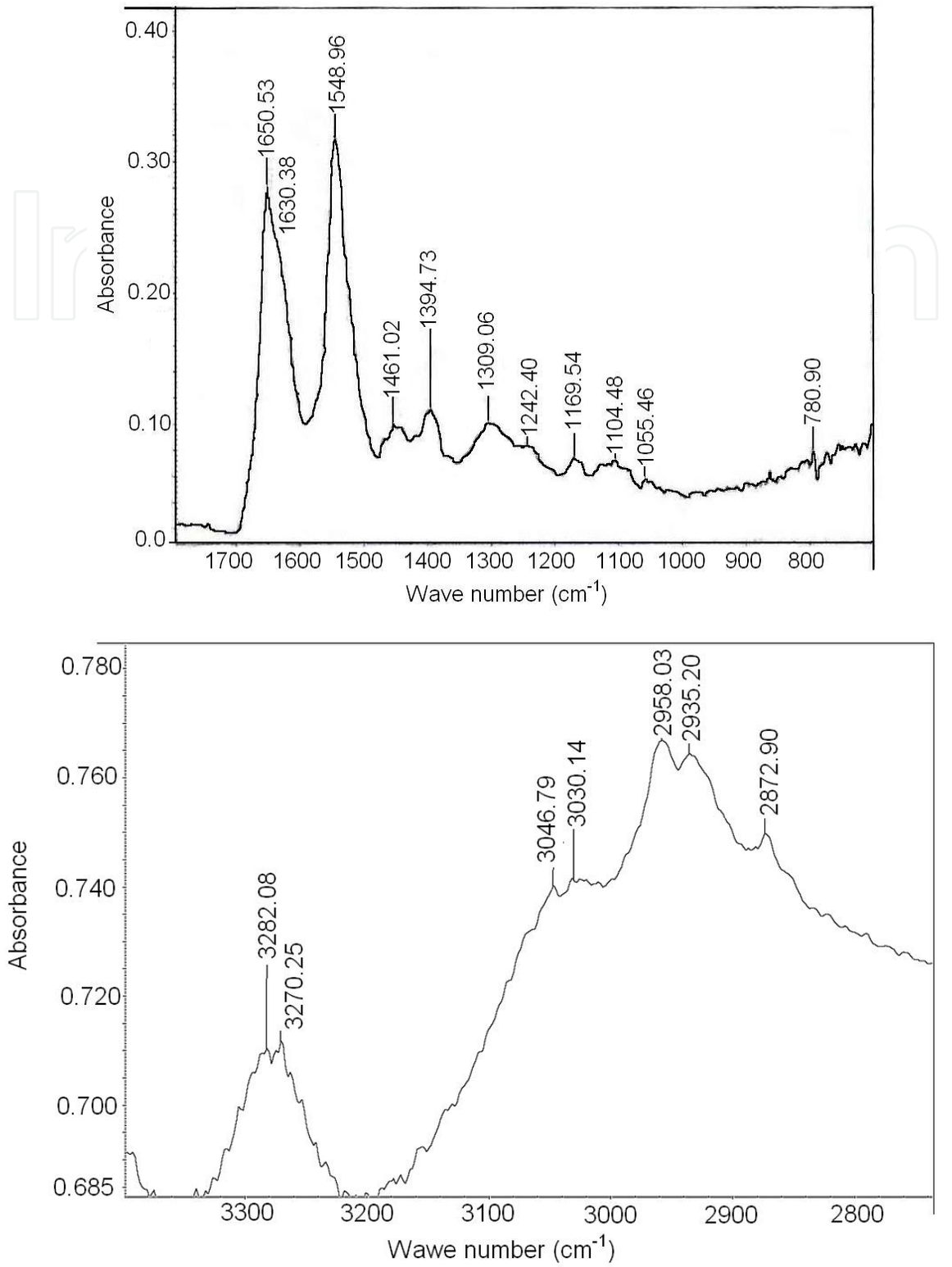

Figure 21. FTIR spectra of human erythrocytes at th addition of cortisol ($C = 3 \cdot 10^{-8}$ M): a. - $\nu = 1000 – 1800$ cm^{-1}, b. - $\nu = 2600 – 3400$ cm^{-1}.

Splitting in the region of 1088 (POC bond) and 3282 cm^{-1} (NH bond) was observed. Splitting of these bands indicates an increasing orderliness in phospholipids and membrane proteins,

respectively. An increase in the fraction of β-structure points to the tangle → β-structure transitions; however, in this case more pronounced is the α-helix → β-structure transition, due to redistribution of intensity between absorption bands at 1650 and 1638 cm^{-1}. The first band corresponds to α-helices, the second one to β-structure [19].

Using the fourth derivative of the absorption band 1600-1700 cm^{-1} the maintenance of elements of the secondary structure in the erythrocyte membranes has been calculated. The results are given in Table 4. This table shows the considerable increase of β-structure under the action of adrenaline. In this case we observe the structural transition tangle → β-structure. However, the increase of α-helices and decrease of tangle under the action of cortisol has been seen. So it can be concluded the structural transition tangle → α-helix took place.

A comparison of IR spectra obtained from ghosts and intact erythrocytes revealed some general regularities: 1) splitting of absorption bands of NH peptide bonds, 2) an increased intensity of absorption bands corresponding to β-structure, 3) splitting of absorption bands corresponding to CH bonds of phospholipids, 4) a frequency shift of some bands (Table 4). However, there is also a distinction related with the appearance of absorption bands at 2870 and 1108 cm^{-1} corresponding to hemoglobin [23]. These bands are shifting when erythrocytes are subjected to the action of hormones.

Conformation	Erythrocyte (control)	Erythrocyte + cortisol $C_{cortis} = 3 \cdot 10^{-8}$ M
α-helical	25%	48%
β-structure	25%	30%
Random coil	25%	22%

Table 4. The quantitative definition of the elements of secondary structure in membrane proteins

Thus, these results suggest that the erythrocyte react to the effect of steroid hormones as a complex liquid-crystalline co-operative system in which nanostructured transitions are irreversible and are closely associated with the functional activity of cells.

8. Thermodynamics of nanostructural transitions in erythrocyte as a liquid crystal system, a relation with the cell function

The application of IR and UV spectroscopy showed that the interaction of steroid hormones with erythrocytes increases the ordering of both the membranes and hemoglobin, which means an increase in negentropy.

E. Schrodinger defined it as

$$-S = k \lg (1/D), \tag{11}$$

where $-S$ is the negative entropy, or negentropy; k is the Boltzmann's constant equal to $3.2983 \cdot 10^{-24}$ cal/deg; D is the quantitative measure of disorderliness of atoms in the system, lg (1/D) is the negative logarithm of D, and 1/D is the measure of orderliness.

However, of prime importance for us is that increasing negentropy is always supported by increasing amount of structural information. This can be expressed by the following equation:

$$-S = k \lg(1/D) + \sum p_i \cdot \log p_i \tag{12}$$

where p_i is the probability of individual events in the system. Thus, the informational component in this equation determines an increase of negentropy in the system and is related with acquisition of new properties.

Developing the concept about a correspondence between negentropy and structural information, we can present the following equality:

$$-S = k \lg(1/D) = \sum p_i \cdot \log p_i \tag{13}$$

Hence,

$$\lg (1/D) = (\sum p_i \cdot \log p_i)/k, \text{ and} \tag{14}$$

$$1/D = 10^{(\sum p_i \log p_i)/k}, \text{ then} \tag{15}$$

$$D = 10^{-(\sum p_i \log p_i)/k} \quad \text{or} \quad 1/10^{(\sum p_i \log p_i)/k} \tag{16}$$

If in the Helmholtz equation for free energy entropy is replaced by D, this gives the following expression:

$$F = U - \frac{T}{10^{\sum p_i \log p_i / k}} \tag{17}$$

Thus, F can be considered as a function of the amount of structural information in a system. This equation is essential for understanding the self-organization processes in living systems, so as the cell. An increase in the amount of structural information determines the transition from liquid crystal to crystal. This may incapacitate a cell from its functioning. It has been already shown that the interaction of steroid hormones increases microviscosity of erythrocyte membranes in the regions of lipid-lipid and protein-lipid interactions. At low concentrations of hormones in the incubation medium, the activity of erythrocyte Na^+,K^+-ATPase even increases, probably due to growing elasticity of the lipid microenvironment of the enzyme, which facilitates structural transitions in the enzyme itself. At high concentrations of hormones (the saturation phase), an increase in microviscosity in the region of lipid-protein interactions makes impossible structural transitions in the enzyme; so, its activity rapidly drops. This determines a dome shape of the enzyme activity curve. Since erythrocyte is a liquid crystal cooperative system, changes occur not only in the activity of Na^+,K^+-ATPase of erythrocyte membranes, but also in the state of cell hemoglobin, its ordering and ability to bind oxygen.

It seems interesting to compare changes in liquid crystals with those occurring in solid crystals in the fields of external action.

Destruction of solid and liquid crystals increases the molar volume [24, 25].

A dependence of the Gibbs thermodynamic potential F(υ) on the molar volume υ taking into account local zones of different scale stress concentrators is described by the equation:

$$F(\upsilon) = U - TS + p\upsilon - \Sigma\mu_i C_i, \quad (18)$$

where μ_i – chemical potential, C_i – concentration (Fig. 22, [26]) .

At critical values of molar volume υ_i = (1,2…6), the thermodynamic potential F(υ) has local minima. They reflect local nonequilibrium potentials in the zones of different scale hydrostatic tension. Critical values of υ_i correspond to different levels of homeostasis in a deformable solid:

υ_0 is an equilibrium crystal; the initial level of homeostasis;

υ_1 are the zones of stress microconcentrators where dislocation cores are generated; the next level of homeostasis;

υ_2, υ_3 are the zones of stress meso- and macroconcentrators where local structural-phase transitions with the formation of meso- and macrostripes of local plastic deformation take place; the next levels of homeostasis;

υ_4 corresponds to intersection of curve F(υ) with the abscissa. At a further increase of the local molar volume, changes of the Gibbs thermodynamic potential proceed under the conditions of $F(\upsilon) > 0$, and the system becomes unstable. Various forms of material failure appear; solid crystal starts to behave as a liquid one.

$\upsilon > \upsilon_6$ – the existence of two phases is possible: at $\upsilon = \upsilon_5$ – the vacancy phase atom, at $\upsilon > \upsilon_6$ – different thermodynamic levels of the crystal lattice in a deformable solid, different levels of its homeostasis.

Thus, plastic deformation of solid and liquid heterocrystals in the fields of external action is a multilevel process of their destruction, with the corresponding levels of crystal lattice self-organization and levels of its homeostasis, i.e., the destruction via different phases of strengthening (self-organization). On solid crystals this decreases the orderliness and amount of structural information. In liquid crystals this increases the orderliness and amount of structural information i.e. liquid crystal ⟶ crystal transition.

Dependence of Gibbs thermodynamic potential on the molar volume υ and changes in the structural information (I), taking into account local zones of stress concentrators is determined by the expression:

$$F(\upsilon, I) = U - T / 10^{(\sum p_i \log p_i)/k} + p\upsilon - \sum \mu_i C_i \quad (19)$$

These quantitative interrelations underlie transition of the system to a new structural level of homeostasis.

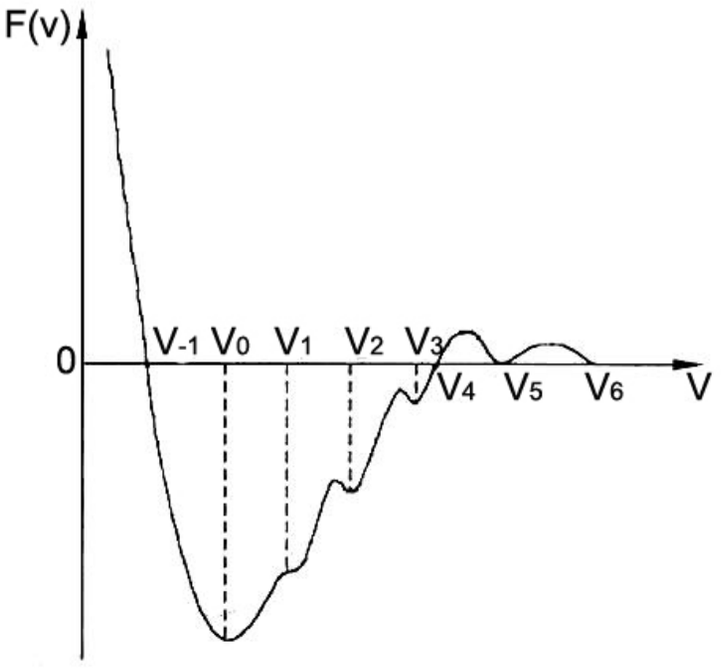

Figure 22. The dependence of the Gibbs thermodynamic potential F (v) from the molar volume v in the light of local zones of stress concentrators of different scales [26].

In biological membranes as liquid crystals, destruction is related with structural transitions and is generally accompanied by increasing structural orderliness (the order → order transition). Earlier [1], it was shown that the action of steroid hormones on erythrocyte membranes disturbs the mechanisms of self-organization that operate in the cells in normal functional condition. The active CO, NH and OH groups of stress hormones interact with CO and NH groups both of proteins and phospholipids in biological membranes. This leads to the formation of complex protein-lipid clusters, where "compressive" hydrophobic interactions are reinforced. Molecularly bound water is displaced to adjacent regions. Here, hydrostatic forces increase the "tensile" tangential stresses. Mobile nanostructural boundaries are formed, along which the biological membranes are destructed. This results in the formation of numerous pores and mesostrips of plastic deformation. In terms of physical mesomechanics, these transformations resemble those developing in solid crystals in the fields of external action (Fig. 23). However, in biological membranes such self-organization may be related even with increasing order and decreasing entropy, but this is incompatible with conditions that determine cell viability. Structural transitions cover the membrane-bound enzymes, transmembrane carriers and hormone receptors. It is reasonable to say that cell membranes go to a new level of homeostasis (self-organization) which is incompatible with life. The nature of life implies dynamics. The cell dies. Here, one can tell about thermodynamic features related with changes in the structure and function (properties) of solid crystals and biological membranes in the fields of external action.

Various structural transitions (phase transitions, nanostructural, etc.) strongly contribute to the functional activity of a cell. These are the transitions like smectic A → smectic C, smectic → cholesteric, and nematic → isotropic state; in proteins, the transitions tangle → β-structure and tangle → α-helix. They all affect the vital characteristics of a cell. I. Prigogine believed that there is "a wonderful analogy between instability of nonequilibrium origin and phase transitions" [27]. This problem is of great interest and deserves special examination.

Thus, on the curve of thermodynamic Gibbs potential versus molar volume F(υ), solid crystals fall in the region of strongly negative values, whereas liquid crystals are located near zero. Structural transformations taking place in the fields of external action draw together the positions of liquid and solid crystals on the functional curve. Morphologically, the destruction patterns of crystals are quite similar (Fig. 9a and b).

Thermodynamically, cells as hierarchic multilevel liquid crystal systems can function only near a zero value of thermodynamic Gibbs potential, i.e. in the region where reversible nanostructural transitions underlying life processes can occur.

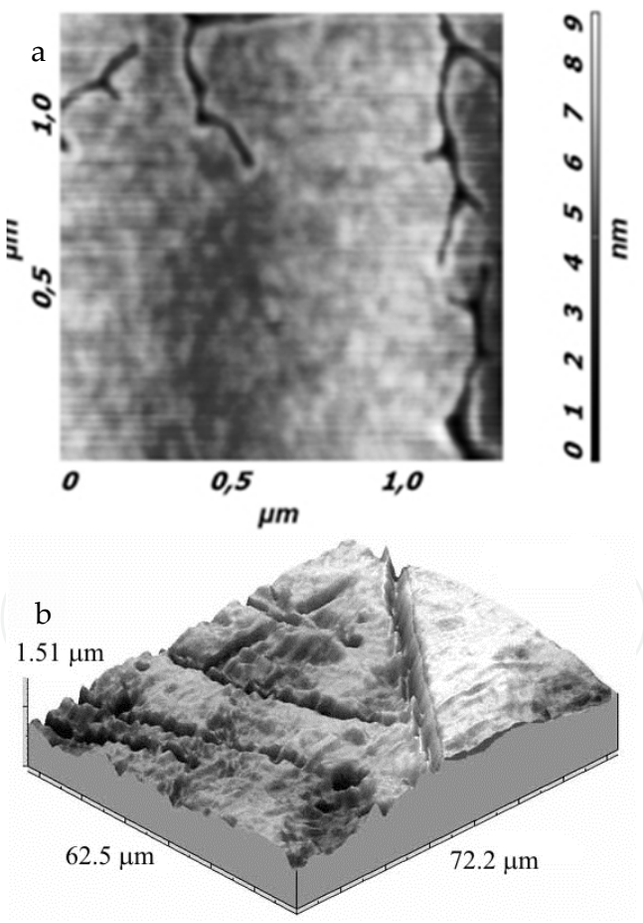

Figure 23. a – Atomic force microscopy. The surface of rat erythrocytes after adsorption of cortisol. Concentration of the hormone is 10^{-6}M. Deep meso-bands with bifurcation are seen; b – Formation of micropore chains along localized-deformation shear-bands. Plate of high-pure aluminum 180 nm thick glued on flat specimen of commercial Al. Alternative bending, T = 293 K; cycle number N = 17.55×10^{6} [26].

Biomembranes are of vital importance in the processes of self-organization of cell metabolism. These processes are transport of organic compounds through cell (plasma) membranes with delivery of nutrients to the cell and removal of their decay products (metabolism); diffusion of gases (O_2, CO_2) through a cell membrane; passive and active ion transport and production of electrochemical potential on the outer and inner surfaces of plasma membranes, and many others. All membranes are liquid crystals. Their behavior in an organism obeys physicochemical laws. The mechanism of their self-organization is the same as that of multilevel systems.

Multilevel systems mean the "hierarchy of scales of shear stability loss of the internal structure of a loaded material in local regions at the nano-, micro-, meso- and macrolevels" [26]. In liquid crystals, this is associated with lipid-lipid, protein-lipid, and protein-protein interactions, i.e. with cooperative behavior of a liquid crystal as a system. The ordering of these crystals as well as the nature of their components is determined by covalent and hydrogen bonds, weak electrostatic and hydrophobic interactions. Shear stability loss of natural liquid crystals depends on structural phase transitions such as the formation of smectic, cholesteric, nematic and isotropic structures and transitions between them. For membrane-bound proteins, states like α- helix, β-structure and chaotic coil are of significance. Structural transitions can be reversible and irreversible. In the latter case, defects are accumulated in liquid crystals, making some functions of the cell membranes unrealizable. The cell dies. These transitions, as a rule, arise on the surfaces of cell membranes and, because of cooperativeness, go deep into their lower levels. They can be also initiated at the inner membrane or particle interfaces and can be related to lipids and proteins. Thus, the case in point is different thermodynamic states of liquid crystals. The low transition enthalpy suggests that the transitions involve low-energy bonds, mainly hydrogen bonds, weak electrostatic and hydrophobic interactions. The external factors capable of changing (disrupting) the interactions are also physicochemical in nature. Among these factors are variations in temperature, pH, electrolyte content, etc. However, they are all of no fundamental character, and the behavior of liquid crystals under external actions fit in the same concept as the behavior of solid crystal does. It is very important for medicine.

As indicated in the report of World Health Organization, cardiovascular pathology, infections and oncological diseases are three main causes of human mortality all over the world [28]. Cardiovascular diseases stand first in this short list. In 2005 they killed 17.5 million people, which constitutes 30% of all deaths in the world. WHO predicts that in 2015 these diseases may take away the lives of 20 millions people. This will be caused mainly by infarctions and strokes, i.e. acute tissue hypoxia.

9. Conclusion

Especially dangerous is myocardial ischemia, which is related with the formation of atherosclerotic plaques within the coronary arteries and a considerable decrease in the blood flow rate. Such mechanism of tissue hypoxia development is typical of the older age groups. However, this pathology may develop also by a different mechanism. Nowadays acute

myocardial ischemia and coronary deficiency are often observed in young people. There are many cases of sudden death that occur in young sportsmen during the competitions [29]. Coronary arteries of sportsmen are free of plaques, nevertheless, acute coronary deficiency develops somehow. Stress hormones and steroid anabolics may be a possible reason.

Today the world is changing very rapidly, and not everybody can adjust to these changes. Chronic stress becomes a wide-spread phenomenon [18]. Such reaction may be very pronounced in anxious persons. This is why cardiac syndrome X is often diagnosed now. Its clinical characteristics include angina chest pain with exertion and ischemic type ST segment depression on electrocardiogram, without angiographic signs of coronary artery stenosis and with normal left ventricle function. It means that acute coronary deficiency of obscure etiology occurs not only in sportsmen, but also among people at large [30].

Cortisol is the main stress hormone. It is a cholesterol derivative, and cholesterol is the essential component of all cell membranes. Of special interest is the erythrocyte membrane. Erythrocyte is a specialized cell that transfers oxygen from lungs to tissues by means of hemoglobin (Hb). In capillaries, oxyhemoglobin HbO_2 decomposes, and O_2 diffuses to the organ and tissue cells. The first obstacle to such diffusion is erythrocyte membrane. Changes in the properties of erythrocyte membrane determine the rate of oxygen diffusion across the membrane. Besides, capillary and erythrocyte may have comparable diameters. Sometimes the erythrocyte diameter happens to be even larger. To go through so small capillary, erythrocyte should have a high plasticity. Structural transformations in erythrocyte membrane under the action of stress hormones may be reflected not only in its plasticity, but also in the mechanism of gas exchange.

In this work, an attempt to elucidate the effect of steroid hormones on the structure of erythrocyte membranes and their physicochemical properties, i.e. the introduction of principles and regularities of physical mesomechanics in biology and medicine provides a deep insight into the mechanism interrelating structure and function of biological membranes, both in the norm and at systemic membrane pathology (upon variation of hormone concentration, temperature, pH, electrochemical potential, etc. has been made.

Thus, from a thermodynamic standpoint, life is the ability of cells to undergo reversible nanostructural transitions near a zero value of thermodynamic Gibbs potential. A loss of this ability leads to cell death and development of pathology.

Author details

L.E. Panin
Scientific Research Institute of Biochemistry SB RAMS, Russia

Acknowledgement

The author is grateful to Dr. Sci. (med.) V.G. Kunitsyn and Ph. D. (phys.-math.) P.V. Mokrushnikov for participation in the preparation of experimental material.

10. References

[1] Panin, L.E.; Mokrushnikov, P.V.; Kunitsyn, V.G. & Zaitsev, B.N. (2010). Interaction mechanism of cortisol and catecholamines with structural components of erythrocyte membranes. *J. Phys. Chem. B.* Vol. 114. No. 29, (Jul. 29, 2010) pp. 9462-9473. ISSN 1520-6106

[2] Hurst, T; Olson, T.H.; Olson, L.E. & Appleton, C.P. (2006). Cardiac syndrome X and endothelial dysfunction: new concepts in prognosis and treatment. *Am. J. Med.* Vol. 119. No. 7, (Jul. 2006) pp. 560-566. ISSN 0002-9343

[3] Rubart, M. & Zipes, D.P. (2005). Mechanisms of sudden cardiac death. *J. Clin. Invest.* Vol. 115. No. 9, (Sep. 2005) pp. 2305-2315. ISSN 0021-9738

[4] Courson, R. (2007). Preventing sudden death on the athletic field: the emergency action plan. *Curr Sports Med Rep.,* Vol. 6, No. 2, (Apr. 2007) pp. 93-100, ISSN 1537-890X

[5] Jorgensen, P.L.; Hakansson, K.O. & Karlish, S.J. (2003) Structure and mechanism of Na+,K+-ATPase. *Annu. Rev. Physiol*. Vol. 65, (May 2002) pp. 817–849. ISSN 0066-4278

[6] Golden, G.A.; Mason, P.E.; Rubin, R.T. & Mason, R.P. (1998) Biophysical membrane interactions of steroid hormones: a potential complementary mechanism of steroid action. *Clin. Neuropharmacol.* Vol. 21. No. 3, (May-Jun. 1998) pp. 181-189. ISSN 0362-5664

[7] Wu, Y.; Hu, Y.; Cai, J.; Ma, S.; Wang, X.; Chen, Y. & Pan, Y. (2009) Time-dependent surface adhesive force and morphology of RBC measured by AFM. *Micron.* Vol. 40. No. 3, (Apr. 2009) pp. 359-364. ISSN 0968-4328.

[8] Kunitsyn, V.G.; Panin, L.E. & Polyakov, L.M. (2001). Anomalous change of viscosity and conductivity in blood plasma lipoproteins in the physiological temperature range. *Int. J. Quantum Chem.,* Vol. 81, (Feb. 2001) pp. 348-369. ISSN 0020-7608

[9] Dawson, R.M.C.; Elliot, D.C.; Elliot, W.H. & Jones, K.M. (1986). *Data for biochemical research.* Clarendon Press, ISBN is absent, Oxford, United Kingdom.

[10] Attallah, N.A. & Lata, G.F. (1968). Steroid-protein interactions studies by fluorescence quenching. *Biochim. Biophys. Acta,* Vol. 168. Issue 2, pp. 321-333, ISSN 0005-2795

[11] Storozhok, S.A.; Sannikov, A.G. & Zakharov, Yu.M. (1997). *Molecular Structure of Erythrocyte Membranes and Their Mechanical Properties,* Tyumen University, Tyumen.

[12] Murray, R.K.; Granner D.K.; Mayes P.A. & Rodwell V.W. (2003). *Harper's Illustrated Biochemistry*, 26th ed., The McGraw-Hill Companies, Inc.

[13] Ooi, T.; Itsuka, E.; Onari, S. et al. (1988). *Biopolymers,* Imanisi Y. (Ed.), Mir, ISBN is absent: Moscow, Russia

[14] Panin L.E., Panin V.E. (2011). Thermodynamics and mesomechanics of nanostructural transitions in biological membranes under stress. *Int. J. Terraspace Science and Engineering*. V. 3. Iss. 1. pp. 3-12. ISSN:1943-3514

[15] Miyazawa, T. & Blout, E.R. (1961) The infrared spectra of polypeptide in various conformations: amid I and II bands. *J. Am. Chem. Soc.* Vol. 83, No. 3 (Febr. 1961) pp. 712-719. ISSN 0002-7863

[16] Semenov, M.A.; Gasan A.J.; Bol'bukh T.V.; et. al. (1996). Hydration and structural transitions of DNA from Micrococcus lysodeikticus in films. *Biophysics*, Vol. 41. No. 5, (Sept. – Oct. 1996) pp. 1007-1016. ISSN 0006-3509.

[17] Discher, D.E., Mohandas, N. & Evans, E.A. (1994). Molecular maps of red cell deformation: hidden elasticity and in situ connectivity. *Science.* Vol. 266. No. 5187, (Nov. 1994) pp. 1032-1035. ISSN 0036-8075.

[18] Shnol, S.E. (1979) *Physicochemical factors of biological evolution,* Nauka, Moscow (Rus.) ISBN 978-91-85917-06-8.

[19] Kunitsyn, V.G. (2002). *Structural phase transitions in erythrocyte membranes, lipoproteins and macromolecules.* Thesis, Dr. Sci. (biol.), Novosibirsk. (Rus.)

[20] Park, Y.; Best, C.A.; Badizadegan, K., Dasari, R.R.; Feld, M.S.; Kuriabova, T.; Henle, M.L.; Levine, A.J. & Popescu, G. (2010). Measurement of red blood cell mechanics during morphological changes. *Proc. Natl. Acad. Sci. U S A*. Vol. 107. No. 15, (Apr. 2010) pp. 6731- 6736. ISSN 0027-8424

[21] Bennett, V. (1984) In: *Cell Membranes: Methods and Reviews*, eds. Elson, E., Frazier, W. & Glaser, L. Vol. 2, Plenum, New York, pp. 149-195.

[22] Storozhok, S. A.; Sannikov, A. G. & Zakharov, Yu. M. (1997) *Molecular Structure of Erythrocyte Membranes and Their Mechanical Properties,* Tyumen Gos. University: Tyumen.

[23] Wolkers, W.F.; Crowe, L.M.; Tsvetkova, N.M.; Tablin, F. & Crowe, J.H. (2002). In situ assessment of erythrocyte membrane properties during cold storage. *Mol. Membr. Biol.* Vol. 19. No. 1, (Jan-Mar 2002) pp. 59-65. ISSN 0968-7688

[24] Panin, L.E. & Kunitsyn, V.G. (2009). Mechanism and thermodynamics of multilevel structural transitions in liquid crystals under external actions. *Physical Mesomechanics*, Vol. 12. No. 1-2, (Jan. – Apr. 2009) pp. 78-84. ISSN 1029-9599

[25] Panin, L.E. (2011). Thermodynamics and mesomechanics of nanostructural transitions in biological membranes under the action of male sex hormones. 13-th International conference on mesomechanics. Vicenza, Italy, 6-8 July 2011. Eds. G.Sih, P. Lazzarin, F. Berto. p. 48-51.

[26] Panin, V.E. & Egorushkin, V.E. (2008). Nonequilibrium thermodynamics of a deformed solid as a multiscale system. Corpuscular-wave dualism of plastic shear. *Physical Mesomechanics*. Vol. 11. No. 3-4, (May - August 2008) pp. 105 – 123. ISSN 1029-9599.

[27] Nicolis, G. & Prigogine, I. (1979). *Self-Organization in Non-Equilibrium Systems. From Dissipative structures to Order through Fluctuations*, Mir, Moscow, Russia.

[28] Vermel', A.E. (2006). Cardiac syndrome X. *Klin Med (Mosk).* Vol. 84. No. 6 (Nov.–Dec. 206) pp. 5-9. ISSN 0023-2149. Russian.

[29] Montagnana, M.; Lippi, G.; Franchini, M.; Banfi, G. & Guidi, G.C. (2008). Sudden cardiac death in young athletes. *Intern Med.* Vol. 47, No. 15, (Aug. 2008) pp. 1373-1378, ISSN 0918-2918

[30] Panin, L.E. & Usenko, G.A. (2004). *Anxiety, adaptation and prenosological clinical examination*. SB RAMS, Novosibirsk, ISBN 5-93239-050-6 (Rus.)